

**Prevention of loss of drilling fluids and formation damage when drilling  
through high permeability formations**

By  
Emil Høgmo

Bachelor's thesis  
Presented to the Faculty of Science and Technology  
The University of Stavanger

THE UNIVERSITY OF STAVANGER

JUNE 2023

## **Foreword**

The laboratory research presented in this thesis was conducted at EMC's (European Mud Company) lab located in Forus, Stavanger.

## **Acknowledgement**

I would like to extend a big thank you to my supervisor Karl Ronny Klungvedt for his excellent guidance throughout this research process. Always providing with his good mood, profound knowledge, input, advice, and laying the foundation for a superb learning experience. He has been crucial throughout this process. I would also like to thank Jan Kristian Vasshus for his great contribution. By facilitating optimal testing conditions in the lab and consistently sharing advice, positivity, inspiration, and motivation. It's all been appreciated. Bjørn Berglind was a pleasure to work alongside for a few weeks in the lab. He provided with his expertise and insight from his inspiring career.

Furthermore, I would like to thank my supervisor, professor Arild Saasen for his shared knowledge and contribution to both the theme and relevant design of this thesis in the early stages, as well as providing this opportunity for me.

## **Abstract**

In order to avoid kicks and the potential for a well blowout, it is necessary to maintain the drilling fluid pressure above the pore pressure of the formation. However, doing so may result in fluid loss due to the fluid being forced into the porous formation and, in some cases, lost circulation caused by excessive pressure that surpasses the formations fracturing pressure. In both scenarios, fluid can migrate into the formation, potentially causing damage.

Fluid loss is an essential aspect of drilling fluids used in the drilling process. Fluid loss refers to the amount of fluid that gets lost or absorbed into the formation while drilling, which can lead to damage to the formation, inability to control pressure, and a reduction in the effectiveness of the drilling fluid. Inadequate control of fluid loss during drilling can lead to decreased productivity, cost overruns, and environmental issues. The drilling fluids ability to reduce fluid loss is an essential factor in maintaining wellbore stability, controlling formation pressures, and avoiding lost circulation problems. To prevent excessive fluid loss, drilling fluids are designed to form a filtercake on the formation's surface, which helps control the fluid loss rate and prevent the formation from being damaged. This filtercake is formed by fine particles of the drilling fluid that get deposited on the surface of the formation, creating a barrier that restricts the fluid loss rate. The amount of fluid loss depends on several factors such as the permeability of the formation, the type of drilling fluid used, the temperature and pressure conditions, and the drilling speed. To maintain optimal drilling conditions, it is crucial to monitor fluid loss and adjust the drilling fluid properties accordingly.

The main focus of this study was to evaluate the relationship between the fluid loss of different drilling fluids following HTHP tests, and an analysis of the respective filtrate that could potentially cause formation damage. An analysis of the filtrate following fluid loss tests, could provide important rheological data that would give extended knowledge of the drilling fluid properties and capabilities. An alternative method for analyzing the fluid filtrate was used for this research. By flowing the filtrate through a needle, the viscosity was calculated at different shear rates. The results show how both spurt loss and overall fluid loss filtrate behaves after both filter paper, and ceramic disc fluid loss tests.

## **Nomenclature**

ECD – Equivalent circulating density  
BHA – Bottom hole assembly  
PSD – Particle size distribution  
HTHP – Hight temperature High pressure  
WBM – Water based mud  
OBM – Oil based mud  
LCM – Lost circulation material  
NIF – Non invasive fluid  
UF – Ultra fine  
AHR – After hot rolling  
BHR – Before hot rolling  
RPM – Revolutions per minute  
FL – Fluid loss  
CFL – Coefficient of fluid loss  
SL – Spurt loss  
RPF – Relative plugging factor  
XF – Extra Fine  
AUF – Auracoat Ultra Fine  
AUM – Auracoat Medium  
AUX – Auracoat Mix

## List of Contents

Foreword.....	2
Acknowledgement .....	3
Abstract.....	4
Nomenclature.....	5
List of Contents.....	6
List of Figures.....	8
List of Tables .....	10
1 Introduction.....	11
1.1 Objective.....	16
2 Methodology.....	17
2.1 Fluid preparation & mixing .....	17
2.2 Rheology.....	22
2.3 Fluid loss.....	23
2.3.1 Fluid loss; filter paper.....	24
2.3.2 Fluid loss; ceramic disc.....	25
2.4 Formation damage .....	26
2.4.1 Disc mass.....	26
2.5 Calibration of low – volume viscosity (Filtrate analysis) .....	27
3 Results & Discussion.....	29
3.1 HTHP effect on different fluids with different median pore sizes .....	30
3.1.1 Effect on fluid loss.....	30
3.1.2 Effect on disc mass .....	36
3.2 Effect of HTHP on filtrate of internally mixed fluid (Filter paper) .....	37
3.2.1 Filtrate analysis of internally mixed WBM .....	38
3.2.2 Filtrate analysis of internally mixed OBM .....	39
3.3 Effect of HTHP on filtrate from external fluid (Filter paper).....	41
3.3.1 Filtrate analysis of external Field Mud (Filter paper).....	42
3.3.2 Filtrate analysis of external LAB Mud (Filter paper).....	44

3.4 Effect of HTHP on filtrate from external fluid (Ceramic discs).....	47
3.4.1 Filtrate analysis of external Field Mud (120µm & 50µm discs).....	48
3.4.2 Filtrate analysis of external LAB Mud (160µm, 120µm, 180µm & 10µm discs).	50
4 Conclusion .....	52
5 References.....	54
Appendix A - Recipes .....	56
Appendix B – Relevant calculations .....	60

## List of Figures

Figure 1: To the left – Ohaus Pioneer scale weight. To the right – Hamilton Beach Mixer ...	20
Figure 2: To the left – Apera pH910. To the right - Ofite roller – oven #172-00-1-C .....	21
Figure 3: Ofite Viscometer 900 .....	22
Figure 4: To the left, HTHP Ofite Filter Press Cell. With Ohaus Navigator scale weight located underneath. To the right, Ofite Fluid Cell .....	23
Figure 5: Citiva Whatman Filter Paper, 22 $\mu$ m pore size .....	24
Figure 6: Top picture from left to right - 10 $\mu$ m disc, 120 $\mu$ m disc, 160 $\mu$ m and 180 $\mu$ m disc. Bottom picture - DVP EC.20 Vacuum Machine .....	25
Figure 7: Ohaus MB120 Moisture Analyzer, utilized for moisture removal and conclusion of disc mass .....	26
Figure 8: Testing setup - Festo Pressure Regulator LRP-1/4-2.5 and LRP-1/4-0.25, Festo Pressure Sensor SPAN-PO25R and SPAN-P10R, Festo Flowmeter SFAH-10U. B. Braun Omnifix syringe. Needle dimensions (m): Length: 0,046. Diameter: 0,0009 .....	27
Figure 9: Shear rate versus Viscosity for WBM + XF + Auracoat UF + Auraseal + 3.6 $\mu$ m CaCO <sub>3</sub> (Sample 1-2).....	38
Figure 10: Shear rate versus Viscosity for OBM (Sample 3-4).....	39
Figure 11: Shear rate versus Viscosity for External Field Mud (Sample 5-6), with additional power law trendline for Primary filtrate (Field Mud) .....	42
Figure 12: Sample 5, Left picture - Primary filtrate to the left and Secondary filtrate to the right. Right picture - Respective filtercake .....	43
Figure 13: Shear rate versus Viscosity for External LAB Mud (Sample 7), LAB Mud + AUF + AUX (Sample 8) and LAB Mud + AUM (Sample 9) .....	44
Figure 14: Left picture – Primary filtrate to the left, secondary to the right with respective filtercake for LAB Mud (Sample 7), Middle picture - Primary filtrate to the left, Secondary filtrate to the right with respective filtercake for LAB Mud + AUF + AUX (Sample 8) with respective filtercake. Right picture – Primary filtrate to the left, Secondary filtrate to the right with respective filtercake for LAB Mud + AUM (Sample 9).....	46



Figure 15: Shear rate versus Viscosity for external Field Mud, Sample 10 (120 $\mu$ m) and Sample 12 (50 $\mu$ m) .....48

Figure 16: Shear rate versus Viscosity for combined filtrate of External LAB Mud + Auracoat UF + Auracoat Mix for Sample 15 (160 $\mu$ m), Sample 16 (120 $\mu$ m), Sample 17 (180 $\mu$ m) and Sample 18 (10 $\mu$ m) with additional power law trendline for Sample 15 (160 $\mu$ m), Sample 16 (120 $\mu$ m) and Sample 17 (180 $\mu$ m).....50

Figure 17 : From left to right, combined Primary + Secondary filtrate for LAB Mud + AUF + AUX, with respective filtercake for Sample 15 – 18. From left to right - 160 $\mu$ m, 120 $\mu$ m, 180 $\mu$ m and 10 $\mu$ m discs. ....51

## List of Tables

Table 1: Components used in water based drilling fluid samples internally mixed. ....	18
Table 2: Components used in oil based drilling fluid samples internally mixed. ....	19
Table 3: Fluid loss results, Sample 1 – 18, along with relevant calculations. In addition are calculated viscosity range for the filtrate of the respective samples presented. ....	32

## 1 Introduction

During the construction, drilling and optimization of a well, a key component is the drilling fluid. As claimed by NORSOK D-010, the drilling fluid acts as the primary barrier of the wellbore, but it also needs to satisfy a certain well barrier acceptance criteria.<sup>1</sup> The fluids journey after mixing, starts with being pumped downhole entering the drill string, and through the nozzles of the drill bit at high shear rates. During this process, one of the many key attributes of the drilling fluid goes into play, to lubricate, cool and clean the drill bit. When drilling a well, it is desirable to open new formation at the bottomhole area with as much force as necessary. With the help of the relative high size and diameter relationship between the drill string and the smaller nozzles, it results in a high velocity differential. The drilling fluid therefore has a much higher velocity and shear rate when going through the nozzles of the bit, than when it is transported through the drill string. This jetting effect contributes to a high rate of penetration. The smaller rock pieces created, as the drill bit plows its way into the formation, is called cuttings. It is of great importance during the drilling process, to get these dispersed cuttings suspended. The drilling fluid is designed to have sufficient viscosity at relevant shear rates, so that the cuttings are suspended in the fluid, and transported to the surface through the annulus. A so-called shear thinning fluid will contribute with a lower viscosity at higher shear rates. In the areas where the shear stress is high, the result is a low viscous fluid, like in the drill bit. In contrast, the fluid shear stress is lower, and the viscosity is higher when the fluid is flowing up through the annulus and transporting the cuttings. The rheological aspect of a still standing fluid in the annular space is also important when there is a stop in circulation. A defined gel strength is required to prevent sagging of cuttings and weighting agents.

Among the drilling fluids many key purposes, a standout factor is to keep the borehole stable, prevent kicks and blowout. In other words, the drilling fluid must control the pressure in the well.<sup>2</sup> To control the pressure in the well, it must be maintained a drilling fluid with such density, equivalent circulating density (ECD), that it results in a higher hydrostatic pressure in the well, than the pore-pressure in the formation. It is desirable that the drilling fluid-pressure is above the pore-pressure, to avoid influx of formation fluids and in the

---

<sup>1</sup> Norsok, 2013, D-010, "Well integrity in Drilling and Well Operations," Standards Norway, Rev 4.

<sup>2</sup> Guan, Z., Chen, T., Liao, H. (2021). Well Control. In: *Theory and Technology of Drilling Engineering*. Springer, Singapore. [https://doi.org/10.1007/978-981-15-9327-7\\_6](https://doi.org/10.1007/978-981-15-9327-7_6)

wellbore, so that the borehole wall receives the necessary support. However, the pressure cannot be as high that it causes the formation to fracture. ECD, the effective density of the circulating fluid, can be defined as the pressure drop in the annular space combined with the measured mud density of the fluid. This must be cautiously balanced, by keeping the drilling fluids ECD between the pore-pressure and the fracture-pressure. If not, the already created hole with the help of physical laws, will inflict the situation with its formation pressure, trying to influx the hole.

When flowing through the drill bit, the drilling fluid gets subjected to relatively high thermodynamical and mechanical exposure. Increasing temperature and mechanical wear on the fluid will affect its rheological properties and the integrity of the particles within it. Before using the drilling fluid in an operation, it might be a difficult task to put the fluid through a characteristic environment as the field circumstances for optimization of the fluid. Hot rolling of the fluid at a certain length of time at reference conditions as in the formation being drilled, is now a widely used technique during testing of the mud to give a good approximation of the fluids mechanical change. Broadening the testing method to an even more representable appearance of the mud, Klungtvedt and Saasen (2022) took it a step further by using a threaded steel rod combined with the fluid in the hot rolling cell to simulate the mechanical degradation before fluid loss tests.<sup>3</sup> After comparing the fluids, both hot rolled with steel-rod and without, they found that the method for applying mechanical shear in the hot-rolling process, strongly differentiated the sealing performance relative to the samples without mechanical wear. The following thesis will use the same approach for hot-rolling before fluid loss tests for drilling fluids, together with a fluid filtrate analysis.

By drilling with an ECD above the pore-pressure, the fluid will migrate into the pore openings in the formation. The result is filtration loss. It is a goal, to create a thin tight filter cake on the well wall, so that we get as little drilling fluid filtrate as possible lost into the formation. Fluid loss will be a result of not maintaining a thin and tight filter cake. The friction force applied to the Bottom Hole Assembly (BHA) will also be affected of the

---

<sup>3</sup> Klungtvedt, K. R., & Saasen, A. (Dec 2022) Comparison of Lost Circulation Material Sealing Effectiveness in Water-Based and Oil-Based Drilling Fluids and Under Conditions of Mechanical Shear and High Differential. *Journal of Energy Resources Technology*. Vol.144, Issue 12

thickness of the filter cake. If the filtercake has a high permeability, it will grow in thickness and may eventually lead to differential pressure sticking, or a stuck-pipe case. In fact, many key elements of the filter cake properties will have an impact on the fluid invasion into the drilled formations, hence affecting the formation productivity according to Ba ger et al.,(2013)<sup>4</sup> and Li & He (2015)<sup>5</sup>. Permeability, porosity, toughness, thickness, structure, and particle size distribution (PSD) will accordingly play a role.

The problem with fluid loss, is that it entails formation damage. On a deeper level, the drilling fluid may contain various amounts of fines and additives, such as drilled solids and polymers.<sup>6</sup> These may be transferred with the filtrate into the nearby formation. This may result in plugged pores, and hence cause a decreased formation permeability. Results of reduced permeability may be costly, as it comes with poor production efficiency and affecting financial aspects rapidly. So, a low fluid loss is considered desirable, to prevent formation damage. To fully understand the role of the fluid filtrate, it is also important to understand the content of the fluid filtrate, as the particles within will impact the degree of permeability reduction.

It is therefore necessary to design the drilling fluid, so that the fluid loss is low. The research conducted for this thesis has been conducted only on static fluid loss test, using both filter paper, and ceramic discs of various pore sizes. An alternative method was introduced to analyze the fluid filtrate from High temperature high pressure (HTHP) tests.

Static fluid loss tests are a main part of a drilling operations weekly schedule, to get the measure of the drilling fluids capability of sealing off permeable formations. By performing tests on ceramic discs, with different median pore sizes, it is attainable to measure the mass difference of the discs. Thereby also acquire an indicator of particle invasion into the near

---

<sup>4</sup> Ba Geri, B. S., Al-Mutairi, S. H., Mahmoud, M. A., Different Techniques for Characterizing the Filter Cake. (2013). *Paper presented at the SPE Unconventional Gas Conference and Exhibition, Muscat, Oman, January 2013*. <https://doi.org/10.2118/163960-MS>

<sup>5</sup> Li, D., He, W., Journey Into Filter Cakes: A Microstructural Study (2015). *Paper presented at the International Petroleum Technology Conference, Doha, Qatar, December 2015*. <https://doi.org/10.2523/IPTC-18246-MS>

<sup>6</sup> Civan, F. Reservoir Formation Damage (2020), *Gulf Professional Publishing: Waltham, MA, USA, 2020*; pp. 1–6, ISBN 978-0-12-801898-9.

wellbore region.<sup>7</sup> An augmentation of this method is to also measure the permeability difference of the discs, hence gaining an extended knowledge of the prospective formation damage, as exhibited by Klungtvedt and Saasen (2022).<sup>8</sup> The use of filterpapers in static fluid loss tests are not as broadly documented as ceramic discs, however ensuing a different story of the drilling fluids capabilities. Experimental research conducted by Alvi et al (2020).<sup>9</sup>, resulted in reduced filtration loss measured on filterpaper, by adding 0,5 wt % iron ioxide nanoparticles to an oil – based drilling fluid. In a sequence of experiments, such filtration loss was nearly halved. These additions also appeared to have formation strengthening effect. Research done by Nelson (2009)<sup>10</sup> revealed that reservoir sandstones typically had pore-sizes exceeding 20  $\mu\text{m}$ , accompanied by pore-throat openings greater than 2  $\mu\text{m}$ . The study also suggested that testing sandstone reservoirs on 20  $\mu\text{m}$  ceramic discs could be indicative of numerous reservoir formations. This thesis will evaluate if testing on filter paper with 22 $\mu\text{m}$  pore size could provide a similarly representative result.

Not enough studies have gone deeper into the filtrate volume following fluid loss tests, that goes into the formations. Klungtvedt et al (April 2023),<sup>11</sup> conducted an experimental analysis, to evaluate the contents of the fluid filtrate relative to the drilling fluid before application. By utilizing a series of tests inclusive of, turbidity, salinity, conductivity, and refractive index (BRIX). Every component hence made a distinctive “fingerprint” concerning relative readings on the various parameters studied. Using this procedure, it was possible to approximate the relative polymer concentrations in the fluid filtrates. This was measured by calculating the BRIX value, and then subtracting the BRIX value, derived from other constituents in the fluid filtrate.

---

<sup>7</sup> Klungtvedt, K. R., Saasen, A., Vasshus, J. K., Trodal, V. B., Mandal, S. K., Berglind, B., Khalifeh, M., 2021, «The Fundamental Principles and Standard Evaluation for Fluid Loss and Possible Extensions of Test Methodology to Assess Consequences for Formation Damage,” *Energies*, 18(8), p. 2252

<sup>8</sup> Klungtvedt, K. R., Saasen, A., 2022, « A Method for Evaluating Drilling Fluid Induced Permeable Formation Damage,” *Journal of Petroleum Science Engineering*, 213, p. 110324

<sup>9</sup> Alvi, M. A. A., Belayneh, M., Fjelde, K. K., Saasen, A., and Bandyopadhyay, S., 2020, “Effect of Hydrophobic Iron Oxide Nanoparticles on the Properties of Oil-Based Drilling Fluid,” *ASME Journal of Energy Resources Technology*, 143(4), p. 043001

<sup>10</sup> Nelson, P.H., 2009. Pore-throat sizes in sandstones, tight sandstones and shales. *Am. Assoc. Petrol. Geol. Bull.* 93, 329–340. NO. 3 (March 2009).

<sup>11</sup> Klungtvedt, K.R., Saasen, A. « The Role of Particle Size Distribution for Fluid Loss Materials on Formation of Filter- Cakes and avoiding Formation Damage”, *Journal of Energy Resources Technology*, April 2023 Vol.145., DOI: 10.1115/1.4056187

The following study will involve an alternative method for measuring the fluid filtrate viscosity after a fluid loss test. Thereby getting a deeper understanding of the viscosity compared to shear rate when it comes to primary and secondary filtrate. In other words, getting a deeper understanding of the functionality and content of the drilling fluid that functions as the spurt loss, and would get knocked into the potential formation. And the secondary filtrate, which might be more or less, alike the primary filtrate when it comes to a viscosity versus shear rate profile.

## 1.1 Objective

The objectives of the study were to evaluate:

- How HTHP fluid loss testing on filterpaper of different grades, potentially could provide rheological information of the fluid filtrate, and hence provide information about particle or polymer invasion into porous formations. Thus provide a broader understanding of the the drilling fluid, and implications for formation damage.
- How a separation between primary and secondary filtrate during fluid loss testing, could provide information regarding potential rheological differences.
- How addition of cellulose based particles and degradation would affect the sealing capabilities of ceramic discs with different median pore sizes.



## 2 Methodology

The methods for assessing fluid loss and conducting the respective filtrate analysis, has been performed on about 70 fluid loss tests. Only a few of them will be presented in this study. The drilling fluids tested on, has been mixed and prepared internally, but also external drilling fluid, used in the North Sea by an established drilling company has been tested and analyzed. Both already applied field mud that has been through circulation, and the same laboratory mud, ready to be used pre - circulation.

### 2.1 Fluid preparation & mixing

For the internal drilling fluid tested, both water based (WBM) and oil based muds (OBM) have been mixed. Whereas several additives and components were involved. The components used, will be presented in **table 1** and **table 2** respectively.

When it comes to laboratory experiments for drilling fluids, 350 mL is practiced as 1 lab barrel. This comes in as especially handy during the mixing of the mud, since 1lbs/bbl will be corresponding to 1g measured in the laboratory. Consequently, all the samples internally mixed in this study has been based on this prescription, with 1 sample, equal to 350 mL. The recipes, with consecutive mixing chronology for the actual samples, are shown in Appendix A. As well as potential additives for the external drilling fluid acquired from the outer source drilling company.

Four different cellulose based products produced by European Mud Company were used during testing. Auracoat XF (Extra Fine, hereinafter referred to as XF cellulose), Auracoat UF (hereinafter called AUF, with a  $D_{90} = 75\mu\text{m}$ ), Auracoat Medium (hereinafter referred to as AUM, with a  $D_{90} < 150\mu\text{m}$ ) and Auracoat Mix (hereinafter referred to as AUX, with a particle size range of  $75\mu\text{m} - 200\mu\text{m}$ ).

Table 1: Components used in water based drilling fluid samples internally mixed.

WBM component	Description/functionality
Water, $H_2O$ , Hydrogen oxide	Base fluid.
Soda ash, $Na_2CO_3$ , Sodium carbonate	Balancing alkalinity in fluid.
Caustic soda, $NaOH$ , Sodium hydroxide	Balancing alkalinity in fluid.
Xanthan gum, XC (Barazan)	Increasing viscosity. Load – bearing capacity.
Polymer (N-Dril HT Plus)	Starch. Reducing fluid loss.
Starch (Dextride – E)	Modified Starch. Balancing fluid loss.
$MgO$ , Magnesium oxide	Preventing radical pH reduction. Especially during hot rolling. Balancing alkalinity in fluid.
Salt, $NaCl$ , Sodium chloride	Weighting agent. Density enlarger.
$CaCO_3$ , Calcium carbonate	Bridging agent. Lost circulation material (LCM).
XF cellulose	Used for fluid loss control.
Auracoat Ultra fine (UF)	Cellulose based particles for Non Invasive Fluids (NIF). Formation damage reducer. LCM.
Auraseal	Used for fluid loss control.

Table 2: Components used in oil based drilling fluid samples internally mixed.

OBM component	Description/functionality
Base oil SIP dril 4.0	Base fluid
$CaCl_2$ Brine 30 %	Production rate enhancer. Minimizing formation damage.
Primary emulsifier	Helps impart high-temperature stability to OBM. Helps lower filtration rates. Helps form stable water-in-oil emulsions.
Secondary emulsifier	Helps impart high-temperature stability to OBM. Helps lower filtration rates. Helps form stable water-in-oil emulsions.
Lime, $Ca(OH)_2$	Stabilizing ingredient.
Organophilic clay	Gelling ability, used to seal rock fractures in the borehole. Increases the yield point and low shear viscosity of the fluid.
Gilsonite	Used for fluid loss control. Improves drilling efficiency and wellbore stability.
Organophilic lignite	Used for filtration control.
$CaCO_3$ , Calcium carbonate (50/50<53 & D50=50 $\mu$ m)	Bridging agent. Lost circulation material (LCM).

Each element present in the mixing of the drilling fluids, were weighed using an Ohaus Pioneer weighing scale. The following mixing was carried out, in a Hamilton Beach Mixer. Both instruments shown in **figure 1**.

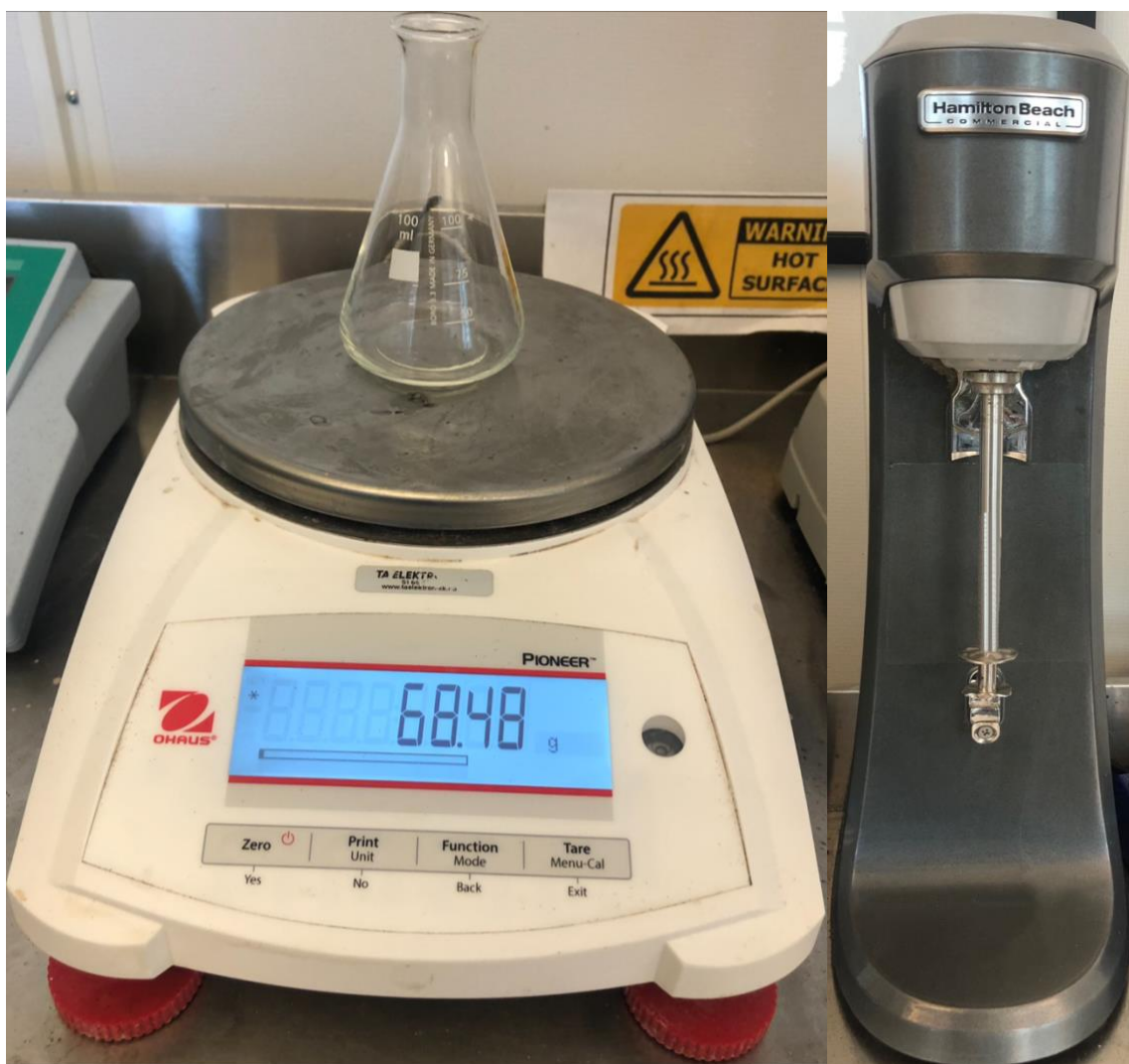


Figure 1: To the left – Ohaus Pioneer scale weight. To the right – Hamilton Beach Mixer.

Following mixing, the pH was measured to control that the fluid contains a certain stable viscosity. A pH between 9 and 12 was considered as a stable and bearing mud. The pH instrument used was Apera pH910, shown in **figure 2**. A pH of the samples was also controlled AHR (after hot rolling). The drilling fluid samples, for both disc and filter paper fluid loss testing, were then portioned into solid cell containers. Along with the fluid, a threaded steel rod was included in the cell containers, hence providing the mechanical degradation simulated as in a productional situation, along with the degradation naturally inflicted by the temperature. Before then being put in a hot rolling oven for 16 hours at 90 °C in a Ofite roller – oven #172-00-1-C shown in **figure 2**. This time duration and temperature throughout rolling, provides a relevant simulation of the fluid, in context with an on-site

production, when it flows through the circulating structure. Potential tests conducted without hot rolling or without steel rod degradation will be stated. AHR, the samples were again spun for 5-7 minutes to thwart any possible sinking of fluid components throughout hot rolling.



Figure 2: To the left – Apera pH910. To the right - Ofite roller – oven #172-00-1-C.

## 2.2 Rheology

To corroborate the certainty of unaltered rheological properties, the viscosity of the fluid samples was measured BHR (before hot rolling) using Ofite Viscometer 900 shown in **figure 3**. The procedure was again repeated AHR, after the samples were spun. All the measurements were carried out at 49 °C at the following RPM (revolutions per minute) in the following order: 600, 300, 200, 100, 60, 30, 20, 10, 6, 3, 2, 1. Following, with a certain gel strength measurement, carried out after both 10 seconds and 10 minutes with 600 RPM at the duration, and measured at 6 RPM.



Figure 3: Ofite Viscometer 900

## 2.3 Fluid loss

The fluid loss test procedure conducted for both filter paper and ceramic discs, was carried out using a HTHP filter press as shown in **figure 4**. When the filter paper/disc was positioned in the filter press cell along with 150 mL of the drilling fluid, the cell was cautiously inserted into the already warmed up HTHP cell. All fluid loss tests, were carried out at 90°C. The fluid loss logging was for all tests achieved by connecting the Ohaus scale as spotted in **figure 4**, to a computer. Hence, the quantity of fluid measured in grams was logged directly in a excel spreadsheet. The fluid loss was recorded at a 5 second time interval, for 30 minutes. By exploiting this arrangement, both mass and volume could be mapped concurrently. Consequently, providing the density of the filtrate. A nitrogen container connected to the top valve of the filter press cell, was used for applying the desired pressure during fluid loss tests.



*Figure 4: To the left, HTHP Ofite Filter Press Cell. With Ohaus Navigator scale weight located underneath. To the right, Ofite Fluid Cell*

### 2.3.1 Fluid loss; filter paper

The filter papers used during fluid loss testing, are the Whatman filter papers shown in **figure 5**. Produced and manufactured by Cytiva. These filter papers are frequently used for routine applications with medium retention and flow rate. Additionally used for covering a wide range of laboratory applications, and commonly used for clarifying liquids. Fluid loss tests on filter papers, have been conducted on a median pore size of 2,5 $\mu$ m and 22 $\mu$ m. All filter paper tests have been carried out on a pressure differential of 500 psi (3,45 MPa). The assembling of the fluid filtrate was done by placing a graduated cylinder beneath the exit valve of the cell, upon the Ohaus weight. The separation of the primary (spurt loss) and secondary filtrate, were done by accumulating the first 30 seconds of the filtrate, hence providing the primary filtrate. By then switching to a new graduated cylinder, the remaining secondary filtrate was collected for the remaining of the 30 minute test.



Figure 5: Cytiva Whatman Filter Paper, 22 $\mu$ m pore size.



### 2.3.2 Fluid loss; ceramic disc

The ceramic discs used for evaluating fluid loss, was OFITE ceramic discs as presented with examples in **figure 6**. Experiments have been done on a wide range of discs with median pore sizes from 250 $\mu\text{m}$  at the largest, to 10 $\mu\text{m}$  at the smallest. Prior to each fluid loss test on ceramic discs, they have been placed in glass tumbler, soaked in ambient temperature water. Before being put in a vacuum machine for air removal, also shown in **figure 6**. Hence imitating a porous formation. A differential pressure of 1000 psi (6,89 MPa) were applied on the discs, following the same procedure as with filter papers. The collection of the filtrate was also carried out with the same procedure as with filter papers; however, some tests were made with the uncertainty of total loss. Which entailed, that the primary and secondary filtrate would be mixed and not separated. Filtrate analysis from selected tests containing a mixture of primary and secondary filtrate, will also be presented.

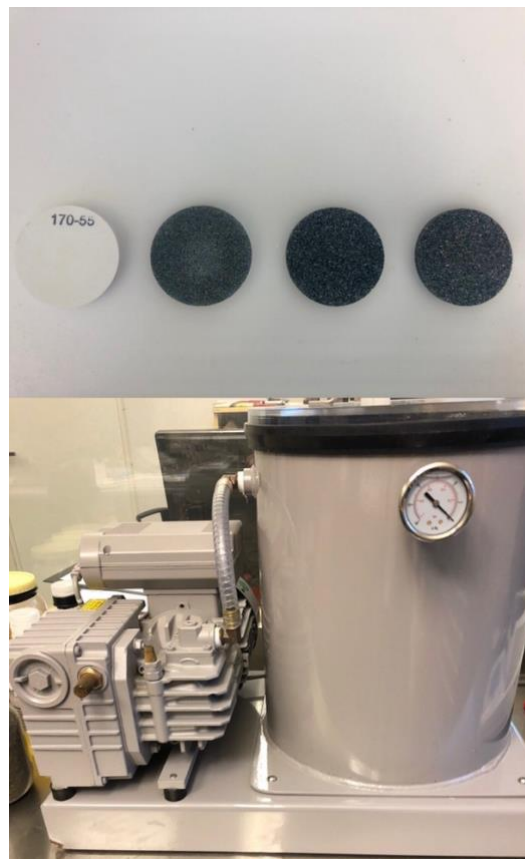


Figure 6: Top picture from left to right - 10 $\mu\text{m}$  disc, 120 $\mu\text{m}$  disc, 160 $\mu\text{m}$  and 180 $\mu\text{m}$  disc. Bottom picture - DVP EC.20 Vacuum Machine

## 2.4 Formation damage

Reduced permeability can be caused by increased mass, which translates into the amount of solid particles, polymers, and fibers from the drilling fluid that remain in the porous medium. The filtercake had to be removed from the ceramic disc in order to study this. A more detailed description of the experimental setup of filtercake removal, is further described by Bergsvik (2022).<sup>12</sup>

### 2.4.1 Disc mass

To investigate and determine if any fluid invasion of the ceramic discs provided any settling of particles i.e., mass increase, the discs were weighed at different junctures during testing. The instrument used for stating the potential disc mass increase are portrayed in **figure 7**. The first measure of the disc was done before the fluid loss test. To conclude with any change in disc mass, the disc was finally measured after filter cake removal.



Figure 7: Ohaus MB120 Moisture Analyzer, utilized for moisture removal and conclusion of disc mass.

<sup>12</sup> Bergsvik, I. S., (2022). Optimizing formulations for reservoir drilling fluids. *Bachelor thesis for University of Stavanger*.

## 2.5 Calibration of low – volume viscosity (Filtrate analysis)

To investigate further the fluid mechanical parameters, rheological properties and potential formation impact of the filtrate, a series of tests were made on the relevant drilling fluid samples following fluid loss tests. Fluid loss test in isolation when controlling a drilling fluid, does not tell a complete story. The viscosity parameters must fit additionally. To determine this, the testing setup used is shown in **figure 8**.



Figure 8: Testing setup - Festo Pressure Regulator LRP-1/4-2.5 and LRP-1/4-0.25, Festo Pressure Sensor SPAN-PO25R and SPAN-P10R, Festo Flowmeter SFAH-10U. B. Braun Omnifix syringe. Needle dimensions (m): Length: 0,046. Diameter: 0,0009

Before implementation of the testing method, the temperature of the filtrate samples was measured. Thereby providing the reference viscosity of the base fluid. The thoroughly distributed filtrate was added in a freshly cleaned and desiccated syringe. By adding the filtrate while the needle is firmly stuck in a piece of silicone, the risk of leakages was maintained. By then connecting the Festo Flowmeter to the syringe with the filtrate inside, with a screw device at the interconnection point. Hence securing no leakages from the air pressure system when the flow rate is measured. The test procedure is then initiated by holding the syringe with the needle horizontally, at a specific fluid elevation of 8mm. This

consistent elevation is a consequence of the pressure difference in the needle. The relevant calculations are shown in Appendix B. By consequently turning the system on at a pressure set beforehand, the test is conducted, and the flowrate (liters/minute) and pressure (bar) is noted. The ejected filtrate then flows into the graduated cylinder initially stored, and the test is ready to be repeated at a different pressure level. The relevant measurements/calculations done for conducting the fluid filtrate analysis were:

- Measured pressure (bar)
- Measured flow (liters/minute)
- Calculated velocity in container (m/s)
- Calculated  $\Delta P$  (pressure differential) in needle (bar)
- Measured fluid elevation (mm)
- Calculated  $\rho$  (density) (kg/m<sup>3</sup>)
- Measured length of needle (m)
- Measured diameter of needle (m)
- Calculated fluid velocity in needle (m/s)
- Calculated Reynolds number (laminar flow if  $< 2100$ )
- Calculated Darcy friction for laminar flow
- Calculated shear stress (Pa)
- Measured temperature of fluid
- Calculated shear rate (1/s)
- Calculated viscosity (Pa\*s)

### 3 Results & Discussion

The following part consists of four segments, whereas each section focuses on a different comparison foundation. The first segment, introduce how the selected 18 drilling fluid samples performed in fluid loss testing, along with principled parameters as relevant comments, coefficient of fluid loss, spurt loss, relative plugging factor and disc mass increase. As well as the calculated viscosity range computed in the fluid filtrate analysis for the respective samples. Section two will present the fluid filtrate analysis following fluid loss tests on filter paper, where the results from internally mixed OBM and WBM with additives will be presented. Section three will investigate the corresponding as in section two, but filtrate analysis following fluid loss tests on filter paper with externally acquired water based drilling fluids, with and without additives. The final section will investigate the filtrate analysis from a combined primary and secondary filtrate from externally acquired water based drilling fluids, as well as one analysis of a separated primary and secondary filtrate. All analysis following fluid loss tests conducted on ceramic discs. **Table 3** displays the designated samples that were tested in the experiments and applied in the following results. Comprehensive information about the designated fluids, are shown in Appendix A.

### 3.1 HTHP effect on different fluids with different median pore sizes

The scope of this segment is to display the effect of fluid loss test, upon the designated fluids with different additives. Relevant factors for fluid loss analysis as spurt loss measurement (0,5 minute), total fluid loss (30 minutes), coefficient of fluid loss, spurt loss constant, relative plugging factor and disc mass increase for ceramic discs will be presented in **table 3**.

#### 3.1.1 Effect on fluid loss

The method for estimating the relevant parameters shown in **table 3** following fluid loss tests, are described by Klungtvedt and Saasen (April 2023) and in Appendix B.

The RPF (Relative plugging factor) is the ratio between spurt loss constant (SL) and the coefficient of fluid loss (CFL), where both SL and CFL are derived from the linear regression model from the respective fluid loss test. This two-factor ratio, makes it possible to get a valid representation of the relative control each factor has in regards of regulating fluid loss, resulting in RPF. RPF is presumably making its most accurate contribution, when comparing fluids with near or equivalent amount of solids concentration, or one fluid on different permeability discs. Nevertheless, all 2,5 $\mu$ m and 22 $\mu$ m filter paper tests, show a healthy RPF, hence highlighted in green in **table 3**. The green/red range in **table 3** for RPF is a direct result from the studies by Klungtvedt and Saasen (April 2023). They found that when the particle D90 to pore size ratio fell below the range of 1,5 – 2,2, the RPF increased rapidly. That indicated that the particles of the fluid did not contribute to creating an external filter cake, but rather enter the formation. Their studies also showed, that as long as the size ratio does not fall below the 1,5 – 2,2 range, the RPF maintains a level in the 20 – 30 range. This could mean that solids invasion is restricted to a certain range, like  $30 \approx RPF$ . That is also the range chosen for the green results presented in **table 3**, with numbers exceeding this categorized as red. As for the disc mass increase which is related to RPF, it has an acceptable green range estimated from the mentioned parameters, choosing 0,050g as the critical point. With disc mass increase values  $>0,050g$  being categorized as comprehensive particle invasion, hence presented in red in **table 3**.

The viscosity for the filtrates presented in **table 3** are derived from low to high shear rates, further graphical representation follows in this chapter.

Table 3: Fluid loss results, Sample 1 – 18, along with relevant calculations. In addition are calculated viscosity range for the filtrates of the respective samples presented.

Sample	Description	Disc/fp pore size (µm)	Pressure (psi)	FL 30s (mL)	FL 30 min (mL)	CFL (mL*T <sup>0,5</sup> )	SL (mL)	RPF (T <sup>0,5</sup> )	Disc mass increase (g)	(Highest to lowest measured) Primary filtrate viscosity (mPs)	(Highest to lowest measured) Secondary filtrate Viscosity (mPs)	(Highest to lowest measured) Pri + Sec filtrate viscosity (mPs)
1	WBM+XF+AUF+AURASEAL+ 3.6µm CaCO3 (Hot rolled with ROD)	22 fp	500	0,57	4,55	0,108	0,22	2,08	-	2,21 – 1,91	1,34 – 1,05	-
2	WBM+XF+AUF+AURASEAL+ 3.6µm CaCO3 (Hot rolled with ROD)	2,5 fp	500	0,34	4,19	0,104	0,002	0,02	-	1,59 – 1,07	1,20 – 1,06	-
3	OBM (Hot rolled with ROD)	2,5 fp	500	0,06	1,17	0,030	-0,04	-1,24	-	-	-	5,84 – 5,14
4	OBM (Hot rolled with ROD)	22 fp	500	0,40	2,57	0,059	0,21	3,57	-	10,97 – 9,72	5,78 – 5,44	-
5	Field Mud (Not hot rolled)	22 fp	500	2,90	10,26	0,201	2,20	10,97	-	9,42 – 4,52	0,98 – 0,87	-
6	Field Mud + Dextride-e (4ppb) + AUF (4ppb) (Not hot rolled)	22 fp	500	0,70	5,70	0,135	0,26	1,93	-	3,98 – 3,09	2,34 – 1,94	-
7	LAB Mud (Hot rolled with ROD)	22 fp	500	1,88	9,67	0,211	1,19	5,65	-	5,73 – 3,12	1,03 – 0,89	-
8	LAB Mud + AUF (4ppb) + AUX (5ppb) (Hot rolled with ROD)	22 fp	500	1,09	8,11	0,189	0,47	2,50	-	4,41 – 2,47	1,21 – 0,95	-
9	LAB Mud + AUM (7ppb) (Hot rolled with ROD)	22 fp	500	1,65	9,96	0,225	0,92	4,10	-	7,80 – 2,79	1,09 – 0,90	-
10	Field Mud (Not hot rolled)	120 disc	1000	6,75	21,25	0,392	5,48	14,0	0,017	2,18 – 1,31	2,04 – 1,53	-
11	Field Mud (Not hot rolled)	160 disc	1000	Total loss	Total loss	-	-	-	0,210	-	-	-
12	Field Mud (Not hot rolled)	50 disc	1000	8,88	24,33	0,418	7,52	18,0	0,002	1,90 – 1,43	2,43 – 2,15	-
13	LAB Mud (Hot rolled with ROD)	160 disc	1000	Total loss	Total loss	-	-	-	0,031	-	-	-
14	LAB Mud + AUF (4ppb) (Hot rolled with ROD)	160 disc	1000	Total loss	Total loss	-	-	-	0,010	-	-	-
15	LAB Mud + AUF (4ppb) + AUX (3ppb) (Hot rolled with ROD)	160 disc	1000	17,44	22,38	0,134	17,01	127,2	0,460	-	-	8,25 – 4,99
16	LAB Mud + AUF (4ppb) + AUX (5ppb) (Hot rolled with ROD)	120 disc	1000	3,28	11,95	0,235	2,52	10,74	0,048	-	-	4,11 – 2,02
17	LAB Mud + AUF (4ppb) + AUX (3ppb) (Hot rolled with ROD)	180 disc	1000	7,81	12,55	0,128	7,39	57,64	0,331	-	-	5,24 – 3,19
18	LAB Mud + AUF (4ppb) + AUX (5ppb) (Hot rolled with ROD)	10 disc	1000	3,72	14,17	0,283	2,80	9,91	0,027	-	-	1,45 – 1,28



There were compelling distinctions in the measured fluid loss among the 18 samples after the HTHP tests shown in **table 3**. For *sample 3* and *4*, the two *OBM* tests included, shows the lowest spurt loss measurement with only 0,06 mL on 2,5 $\mu$ m filter paper and 0,40 mL on 22 $\mu$ m. Additionally, resulting the lowest total fluid loss, with 1,17 mL and 2,57 mL respectively. For *sample 1* and *2*, the internally mixed *WBM*, the fluid loss was also relatively low. 0,34 mL spurt loss and 4,19 mL total for *sample 2* on 2,5 $\mu$ m filter paper. 0,57 mL spurt loss and 4,55 mL total for *sample 1* conducted on 22 $\mu$ m filter paper. Considered that most Oil based muds are formulated to withstand higher temperatures and pressures compared to Water based muds, the differences between these samples were not surprising. But the distinct difference is shown by comparing these tests with the filter papers as foundation. The spurt loss for both *WBM* and *OBM* on 2,5 $\mu$ m is significantly lower compared to 22 $\mu$ m. The reason for this, is the small pore size of the filter paper. Several tests were conducted on 2,5 $\mu$ m filter paper, and the results were consistent. That the small pore sizes were unable to separate the primary (spurt loss) and secondary filtrate good enough. In other words, the spurt loss showed a relatively consistent low volume, as exemplified by *sample 2* and *sample 3*. These two samples do also deliver low spurt loss constants (SL) and relative plugging factors (RPF). The negative values for (*sample 3*) might be explained by several factors. The fact that the filter papers are not pre-wetted, as the ceramic discs are, applies. This makes the tighter filters in the filter papers provide a certain fluid migration time. It takes more time for the fluid to go through the filter, which results in a negative SL and RPF in this instance for *OBM* (*sample 3*). This effect occurs more with *OBM*, because of its loaded, larger water particles that creates the filtercake on 2,5 $\mu$ m filter paper, before the 500 psi pressure is applied. There are no issues related to these negative values. If the filter paper for instance were pre – wetted in the base fluid, the results would be different. It is also important to emphasize, that *OBM* is the least environmental – friendly fluid amongst the 18 samples, although showing a good fluid loss performance. *Sample 1* and *2* are on the other hand a much more suitable fluid to use when it comes to environmental aspects. They do also perform well on the fluid loss test with just a slightly higher volume at both 2,5 $\mu$ m and 22 $\mu$ m, compared to *OBM*.

As the RPF formula suggests, a high value of RPF would signify a fluid loss predominantly influenced by spurt loss, resulting in plugging of the formation. A satisfactory representation of this, is shown by *sample 15* and *17*. Both samples respectively conducted on

160 and 180  $\mu\text{m}$  discs. These tests show a distinctive large spurt loss measurement and spurt loss coefficient, relative to the other samples. These two fluids are similar, but with a different amount of additives. The high value of RPF, could suggest that these two fluids could potentially be optimal in a borehole stabilization situation. However, *sample 15* constituted the second highest fluid loss overall, apart from the tests resulting in total loss.

Another interesting observation is done by looking at *sample 12*. This test resulted in a high spurt loss, but also the highest total fluid loss after 30 min, not considering total losses. This test of the *Field Mud* was conducted on a 50 $\mu\text{m}$  disc, and despite the relatively high total fluid loss, the RPF is considered acceptable with 18,0. It also resulted in a minimal amount of particle invasion, with only 0,002 g disc mass increase. By comparing this result to *sample 15* and *17*, it shows that a high overall fluid loss, does not necessarily correlate to a high RPF and disc mass increase. For the *Field Mud* in *sample 12*, a reason might be the effect of degradation applied to the fluid during production in the North Sea. Hence providing smaller and more affected particles to invade the disc. On the other hand, by looking at *sample 10*, the fluid loss decreases for the *Field Mud*, with an increase in pore size. This might indicate an uncertainty in the fluid, considering degradation, but also what is brought along from the North Sea. The *Field Mud* showed signs of sandstone particles, which might affect the rheological properties of the fluid. By increasing the median pore size to 160 $\mu\text{m}$ , the *Field Mud* resulted in total loss, as shown by *sample 11*. The *Field Mud* were not hot rolled because of its already degraded effect from production.

The total fluid loss of the disc samples on the *Field Mud* and *LAB Mud*, does not necessarily seem to correlate to an increase in median pore size.

By evaluating the *Field Mud* tests conducted on 22 $\mu\text{m}$  filter paper, *sample 5* and *6*, the effect of additives is prominent. Where *sample 5* is the *Field Mud* without additives, *sample 6* is the *Field Mud* with added 4 ppb of ultra fine cellulose based particles (AUF) and 4 ppb of starch (Dextride-e). Where Dextride-e increases viscosity and reduces fluid loss. *Sample 6* resulted in 122% lower spurt loss and 57% lower total fluid loss compared to *sample 5*. Meaning that both the starch and AUF significantly strengthened the *Field Mud* when it comes to fluid loss. *Sample 6* also had a significantly better RPF with 1,93, where *sample 5* had 10,97. This indicates that *sample 6* would provide significantly less formation damage compared to *sample 5*.

The *LAB Mud* showed generally low volumes of both spurt loss and total fluid loss for the tests conducted on 22 $\mu$ m filter paper, *sample 7-9*. The effect of the cellulose based additives (AUF, AUX, AUM) resulted in lower spurt loss for *sample 8 (with AUF and AUX)* and *9 (with AUM)*, but only lower total fluid loss for *sample 8*. All these tests resulted in acceptable RPF.

As for the fluid loss results for the *LAB Mud* from ceramic discs, the results are more different. Naturally, because of the variation in median pore size, but also because of the amount of added cellulose based particles. *Sample 13* and *14*, both tests conducted on 160 $\mu$ m disc, resulted in total loss with barely any particle invasion in the disc. Where *sample 13* was the plain *LAB Mud* and *sample 14* the *LAB Mud + AUF*. By adding larger cellulose based particles to the fluid in the form of AUX, the fluid loss test was feasible and more under control, but high volume of fluid loss either way. In addition, the disc mass increase was significant.

*Sample 17* tested on 180 $\mu$ m disc and *sample 15* conducted on 160 $\mu$ m disc, had the same amount of additives. Interestingly, did *sample 17* deliver lower spurt loss and total fluid loss, but still ended up with a high RPF and disc mass increase. There might be several reasons to this, one might be individual variations and specifications in the ceramic discs. Another might be the AUX particles which is in a wide sized range. Hence might be closer to the 160 $\mu$ m range, causing more plugging and increase to the disc mass relative to the 180 $\mu$ m disc. The AUX particles might also enter the 180 $\mu$ m disc, but gets dislocated during reverse flow of the disc. The fluid loss is generally expected to increase for similar fluids upon larger pore sizes.

The big picture of the fluid loss results conducted on 22 $\mu$ m filter papers, are sufficiently acceptable. However, the lower total fluid loss volume on filter papers compared to the ceramic discs may be explained by the sealing pressure differential, in addition to the lower median pore size. Respectively 500 psi on filter papers and 1000 psi on discs. The pressure carried out on the filter papers are limited to what the filter papers can withstand. The *Field*

*Mud* experimented on, resulted in the highest spurt loss and total fluid loss on filter paper. Resulting in the largest RPF of the filter paper tests.

### **3.1.2 Effect on disc mass**

Another interesting observation upon investigation, is the varying results of disc mass increase among the nine samples tested on ceramic discs.

The largest result in particle invasion was for *sample 15* with 460 mg and *sample 17* with 331 mg. The substantial deviation of disc mass increase compared to *sample 16* and *18*, could be related to the comprehensive spurt loss and insufficient sealing capacity. A potential candidate for invading and settling in the disc, are polymers. The thickening agent of Xanthan gum is a possible polymer that could result in plugging the pores and increasing the mass, because of its extended molecule chains. However, *sample 13-18* are all derived from the same external *LAB Mud*. Hence turning the heads towards the additives. Whereas *sample 15* and *sample 17* consists of the same lesser number of larger sized cellulose based particles added, compared to *sample 16* and *18*. In addition to being tested on discs with a larger median pore size. With a an additive amount differential of just 2 ppb, it is an interesting paradox that a relatively small difference in fiber content, could have such large effect on particle invasion and plugging. Cellulose based particles are essentially included in drilling fluids for prevention of lost circulation, acting as LCM. As well as increasing the sealing capacity. For the *Field Mud (Sample 10 and 12)* there was no significant particle invasion. Only increasing with 0,017 g for *sample 10* and 0,002 g for *sample 12*. A reason to this, might be the extensive mechanical and thermodynamical degradation the *Field Mud* were exposed to during circulation in the wellbore.

### **3.2 Effect of HTHP on filtrate of internally mixed fluid (Filter paper)**

The following segment will provide an insight on the effect of HTHP Fluid loss tests upon the respective filtrate. The filtrate analysis will encircle relevant viscosity parameters. The presented results in this section will consist of *samples 1-4*, where both fluids were internally mixed, and tested on filter paper with pore size of 2,5 $\mu$ m and 22 $\mu$ m. *Sample 1-2* is a water based drilling fluid containing two added fine powdered calcium carbonate additives. 20 ppb of 3,6  $\mu$ m CaCO<sub>3</sub> and 10 ppb Trucarb 10 (10 $\mu$ m). *Sample 3-4* is an oil based drilling fluid, containing 75% oil portion and 25% brine, as well as added CaCO<sub>3</sub>. The complete recipes are presented in Appendix A.

### 3.2.1 Filtrate analysis of internally mixed WBM (Filter paper)

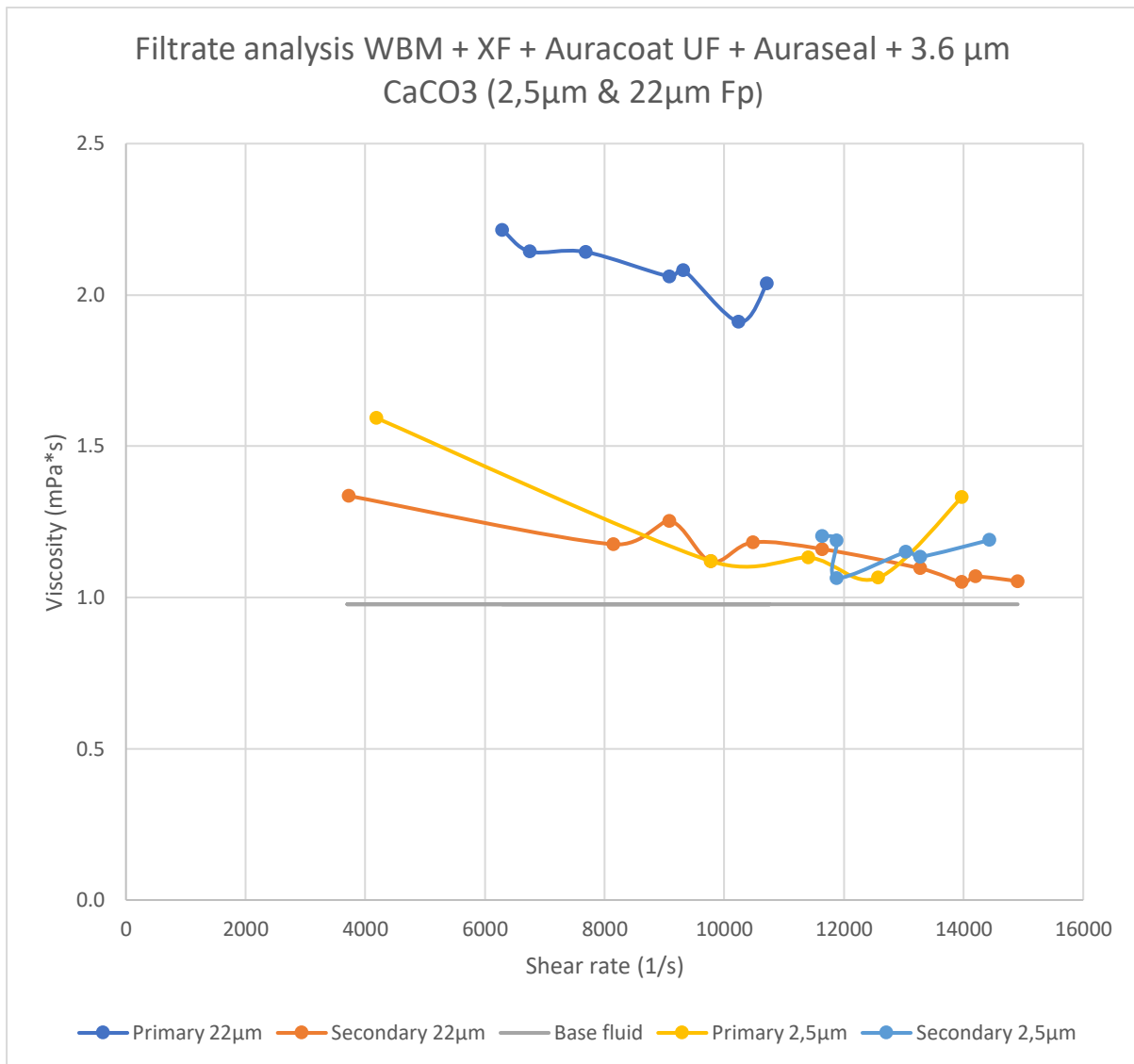


Figure 9: Shear rate versus Viscosity for WBM + XF + Auracoat UF + Auraseal + 3.6  $\mu\text{m}$  CaCO<sub>3</sub> (Sample 1-2).

Sample 1-2 in figure 9 resulted in three filtrates close to the reference viscosity of water (base fluid) measured at 21°C. By measuring the temperature of the filtrate, the reference viscosity (water for WBM) was easily attainable. The primary filtrate for sample 1 conducted on 22 $\mu\text{m}$  filter paper resulted in the highest viscosity and indicates a decreasing path upon increasing shear rate. This could mean that the filtrate is shear – thinning, also called pseudo – plastic. This might illustrate the effect of small structural changes within the fluid. The polymer chain content of the fluid might begin to detangle and align towards the direction of the shear stress, when perturbed enough. Because of the reduced particle contact and more

free space, viscosity will diminish. Which encourages the impression of shear thinning filtrate. From the 22 $\mu$ m filter paper test, the primary filtrate resulted in a 58% higher viscosity compared to the secondary on average measurements. The results also illustrate how the filtrate from the 2,5 $\mu$ m filter paper test (*sample 2*), are unable to sufficiently separate the filtrates compared to the *sample 1*. The two filtrates show some irregularities in the measurements, but the viscosity of the filtrates show more similar properties compared to the filtrates from 22 $\mu$ m.

### 3.2.2 Filtrate analysis of internally mixed OBM (Filter paper)

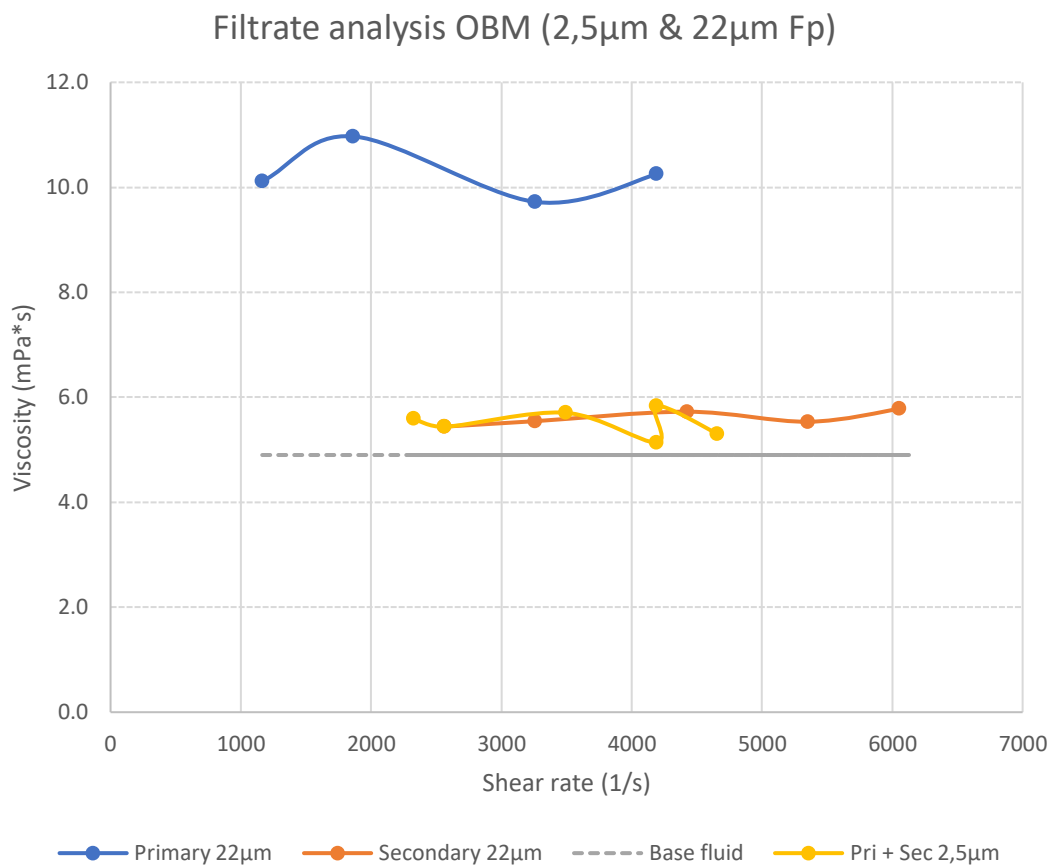


Figure 10: Shear rate versus Viscosity for OBM (Sample 3-4).

The reference viscosity of the base fluid (Sip drill 4.0) was here calculated to be 4,9 cP. **Figure 10** presents the relatively large difference in viscosity for the 22 $\mu$ m filtrates. Compared to the reference viscosity, the primary filtrate stands out with its large viscosity with an average of 10,26 cP. The secondary filtrate shows the more linear trend of the two,

which might indicate a cleaner filtrate. Upon investigation, the viscosity of the secondary filtrate which has an average of 5,61 cP, also seems to remain reasonably stable upon increasing shear rate. This is characteristic for a Newtonian fluid behavior. The more viscous base oil in *OBM* compared to water in *WBM*, is a factor to include in the viscosity results, as the *OBM* also includes some water. On average, the primary filtrate resulted in a 58,6% higher viscosity than the secondary filtrate. For the 2,5 $\mu$ m filtrate, the two of them were combined because of the small primary loss as seen in **table 3** with only 0,06 mL. When the spurt loss is of such small volume, the testing method is unable to measure a reasonable flow rate by applying pressure, because of the low filtrate volume. Because of this, in addition to several tests conducted on 2,5 $\mu$ m with consistently low primary loss and small distinctions between primary and secondary filtrate viscosity, 22 $\mu$ m filter paper was more representable for filtrate analysis. Hence preferred for the remaining fluid loss tests on filter paper. The combined primary and secondary *OBM* filtrate from the 2,5 $\mu$ m test shows a similar trend as the secondary 22 $\mu$ m. The results shows that when the filtercake for *sample 3* has been established, the resulting filtrate is nearly base fluid.



### **3.3 Effect of HTHP on filtrate from external fluid (Filter paper)**

The scope of this section is to evaluate the results from filtrate analysis from an externally acquired drilling fluid, with internally mixed additives. Both operational field mud used for drilling in the North Sea, and LAB mud recently mixed prior to production. All tests have been conducted on 22 $\mu$ m filter paper. The results presented consists of *sample 5-9*. Whereas *sample 5-6* represents the field mud, and *sample 7-9* the LAB mud.

### 3.3.1 Filtrate analysis of external Field Mud (Filter paper)

The choice of regression lines for selected filtrates in the remaining results, have been purely selected based on goodness of fit. As long as the models follows physical laws, and fluid mechanical principles. The reason to this, is to investigate if there is some relationship and consistency based on the best fitted regression model.

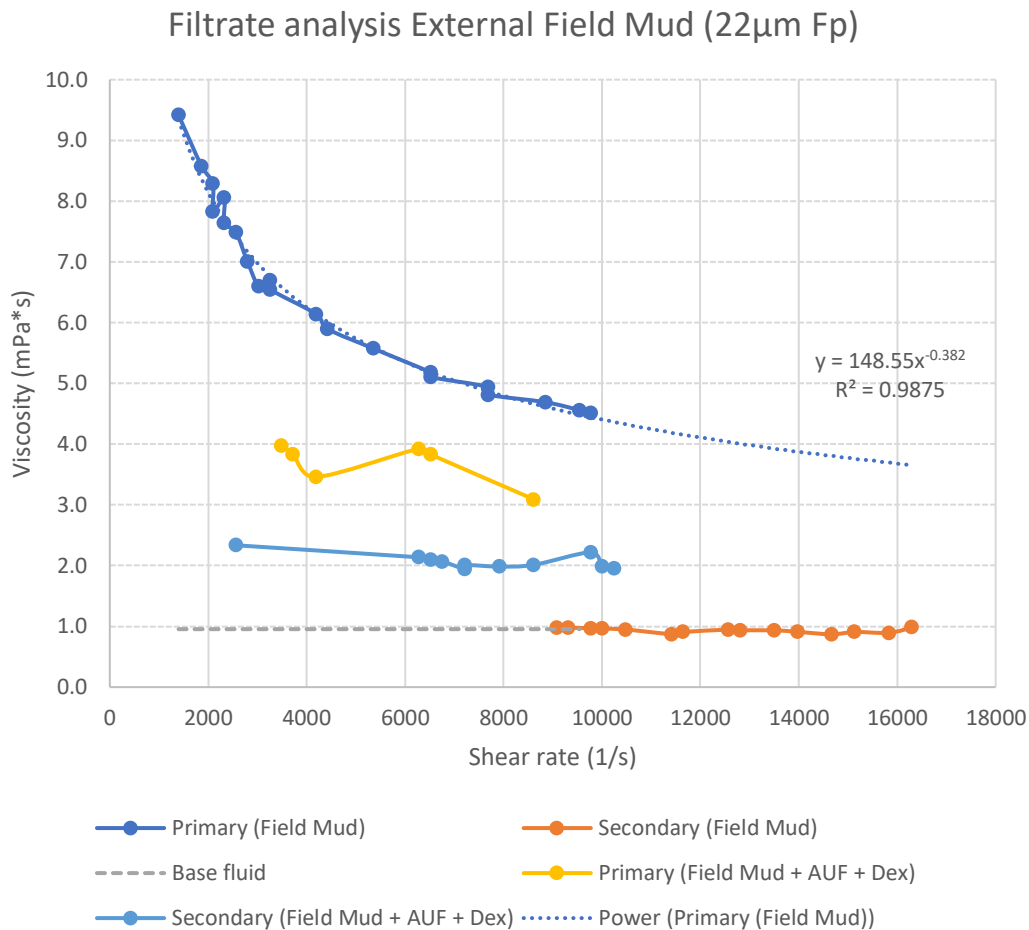


Figure 11: Shear rate versus Viscosity for External field mud (Sample 5-6), with additional power law trendline for Primary filtrate (Field Mud).

**Figure 11** illustrates a unique distinction between the primary and secondary filtrate of the Field Mud without additives, and with added ultra fine cellulose based particles + starch. The *Field Mud* (Sample 5) was only spun in the Hamilton Beach Mixer for 5 minutes and was naturally degraded in the drilling system offshore as described in the introduction, hence not hot rolled. The same for *Field Mud + AUF + Dex*, but the additives were added during

the spinning in the mixer. The secondary filtrate for the *Field Mud* indicates a considerably similar viscosity relative to the reference viscosity of the base fluid at a measured 22°C. Additionally behaving as a Newtonian fluid, with only slight points of deviation upon shear rate. The primary filtrate on the other hand, express a clear power law fluid with a strong 0,9875 on goodness of fit. Substantiating a more evident non – Newtonian filtrate that is shear thinning, and highly viscous compared to the secondary. Representing a noticeable distinction between primary and secondary filtrate.

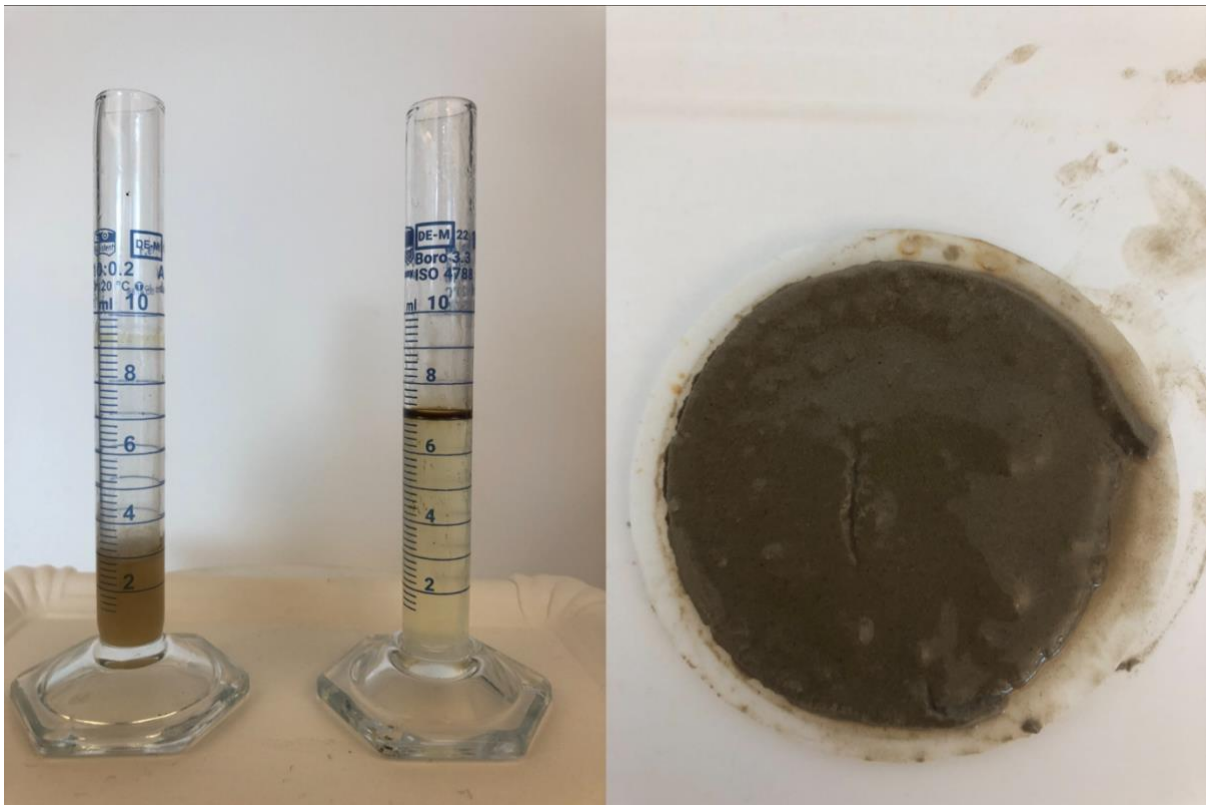


Figure 12: Sample 5, Left picture - Primary filtrate to the left and Secondary filtrate to the right. Right picture - Respective filter cake.

The secondary filtrate in **figure 12**, appears unscientifically to be more transparent relative to the primary filtrate. Which substantiate the theory of a more waterlike filtrate. The primary filtrate additionally showed strong signs of sandstone brought along from the field operation in the North Sea. Which might indicate that also 22µm filter paper could provide a representative of a reservoir formation in reference to the study by Nelson (2009). By adding Auracoat UF and Dextride-e to the *Field Mud*, the viscosity of the secondary filtrate increased as the viscosity of the spurt loss decreased. This is an interesting observation as starch is considered as a viscosity enhancer. It is likely, that the ultra fine cellulose based

particles might have contributed to the viscosity decrease of the spurt loss. *Sample 6* still shows signs of two clearly separated filtrates, although much closer viscosity than the *Field Mud* without added particles and starch. Upon investigation, does the secondary filtrate show a thin layer of black fluid. It might be an addition of emulsifier, or other chemical substance added by the drilling company mixing the fluid.

### 3.3.2 Filtrate analysis of external LAB Mud (Filter paper)

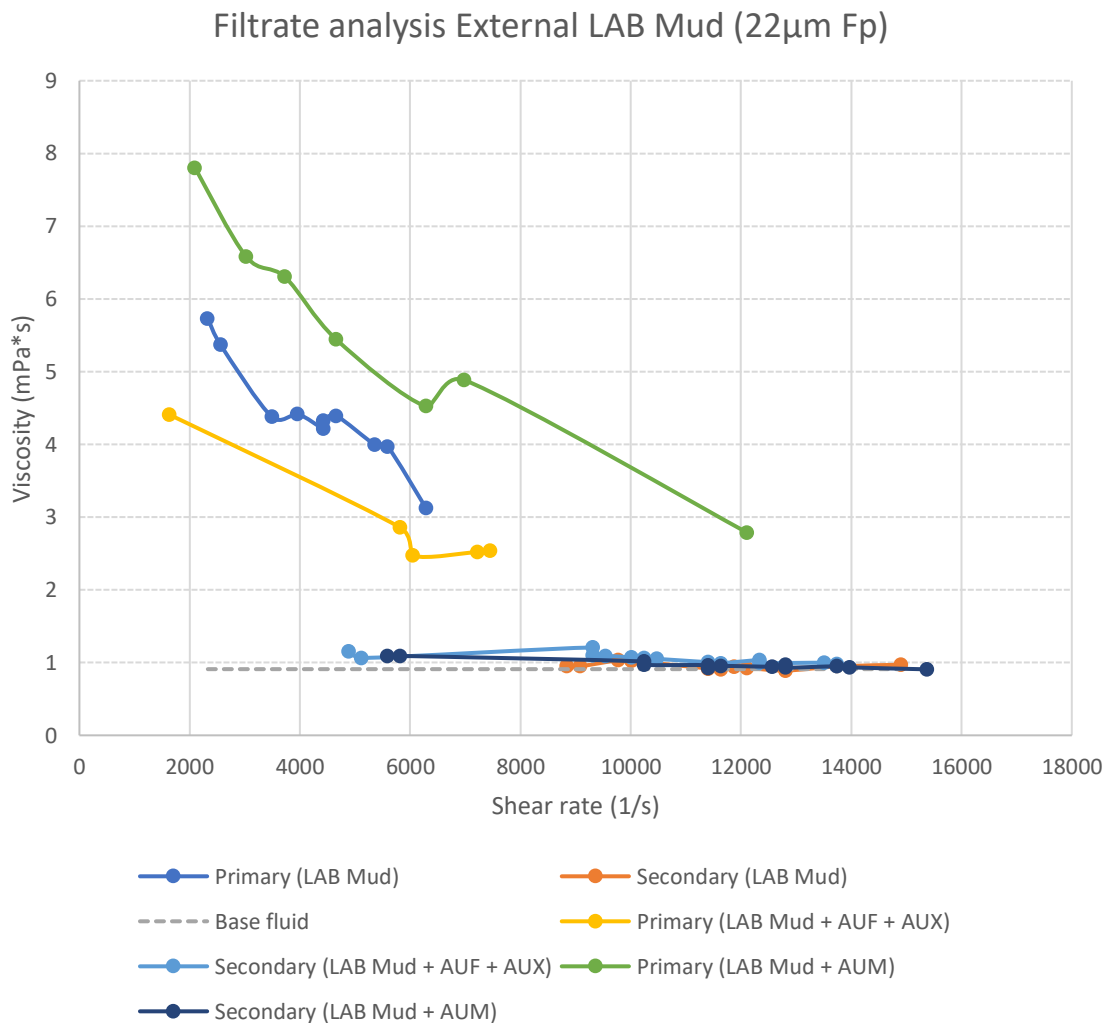


Figure 13: Shear rate versus Viscosity for External LAB Mud (Sample 7), LAB Mud + AUF + AUX (Sample 8) and LAB Mud + AUM (Sample 9).

With the external LAB mud not being exposed to the same thermodynamical and mechanical degradation as the Field mud, *samples 7-9* were hot rolled accompanied with steel rod. An analysis of an untouched LAB mud without additives and with added particles are shown in **figure 13**. The results present again that the primary and secondary filtrate are clearly separated with rheological parameters considered. The secondary filtrate from all three samples, lies close to the line of the reference viscosity of the base fluid at 24°C, with a Newtonian fluid behavior. The large interval of increasing shear stress upon these filtrates does not affect the viscosity significantly, and the trend for all three secondary filtrates seem to be uniform. Interestingly does the primary filtrate also express a shear thinning profile for all three samples. It might also appear that the viscosity of the primary filtrate with increasing shear stress, is decreasing at a larger pace upon shear stress compared to the *Field Mud*.

By the addition of Auracoat Medium (AUM) to the LAB mud (*Sample 9*), particles in a medium range between AUF and AUX, the fluid delivered a higher fluid loss compared to *sample 8*, but still less than the LAB mud without particles. An average viscosity difference of 4,5cP, divided the two filtrates for *Sample 9*, a 139,76% difference. More than *Sample 8* which contained more ultra fine cellulose based particles (AUF) but also larger particles (AUX). It might indicate that the added ultra fine particles in *Sample 8* were retained, and binding with the existing polymers, hence contributing to filter cake development. Resulting in a less viscous primary filtrate compared to the other two samples. The ultra fine cellulose based particles thus decreases the viscosity, which is consistent with the study by Klungvedt and Saasen (April 2023). Substantiated by the results in section 3.3.1. By only adding larger particles (AUM), the viscosity increased. With the *LAB Mud* without additives, having a viscosity profile laying in the middle of the other two samples with additives. By looking at a percentage relation between the two filtrates for the *Lab Mud* on average viscosity measurements, a profound 128% distinction separates.

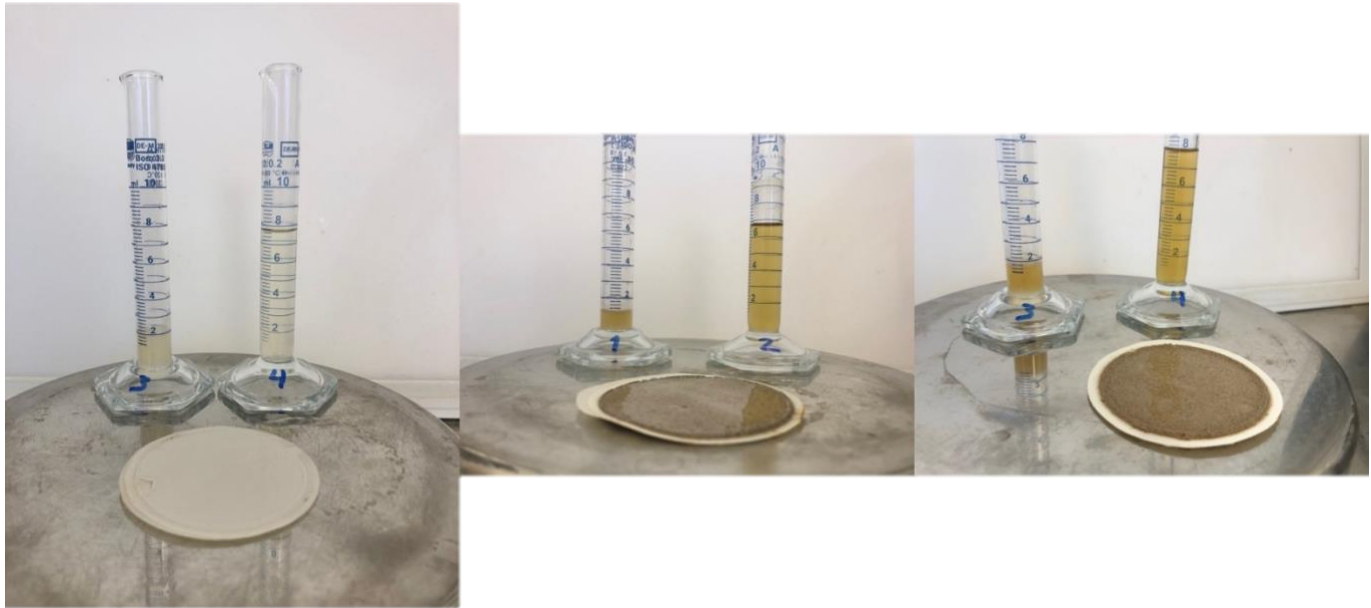


Figure 14: Left picture – Primary filtrate to the left, secondary to the right with respective filtercake for LAB Mud (Sample 7), Middle picture - Primary filtrate to the left, Secondary filtrate to the right with respective filtercake for LAB Mud + AUF + AUX (Sample 8) with respective filtercake. Right picture – Primary filtrate to the left, Secondary filtrate to the right with respective filtercake for LAB Mud + AUM (Sample 9).

**Figure 14** illustrates the well distributed cellulose based particles attached to the filter cake for *Sample 8-9*. A slightly more viscous spurt loss upon visual inspection accounts for all three samples. As all the secondary filtrates resulted as low viscous relative to the primary filtrates, does **figure 14** show that all the secondary filtrates mainly contain dyes from the cellulose based particles. Also here, does the secondary filtrate illustrate a thin discolored layer upon inspection, similar to the *Field Mud*. The complete properties of both the *Field Mud* and *LAB Mud* were unknown during this study.

### 3.4 Effect of HTHP on filtrate from external fluid (Ceramic discs)

The effect of a HTHP fluid loss test conducted on filter paper with separated filtrates has been evaluated. It might also be interesting to see if the rheological behavior of a combined well distributed primary and secondary filtrate will express itself in a certain kind of way. By also investigating the potential viscosity relationship towards the reference of the base fluid. Nine samples both with and without additives were tested on different ceramic discs with different median pore sizes. Where two *Field Mud* analysis without additives were conducted with separated filtrates, and four *LAB Mud* analysis with the same additives with combined filtrates. However, did *sample 15* and *17* contain the same amount of additives. And *sample 16* and *18* the same. Three samples conducted on ceramic discs as seen in **table 3** resulted in total loss, hence no representable filtrate of these tests was analyzed.

### 3.4.1 Filtrate analysis of external Field mud (120 $\mu\text{m}$ & 50 $\mu\text{m}$ discs)

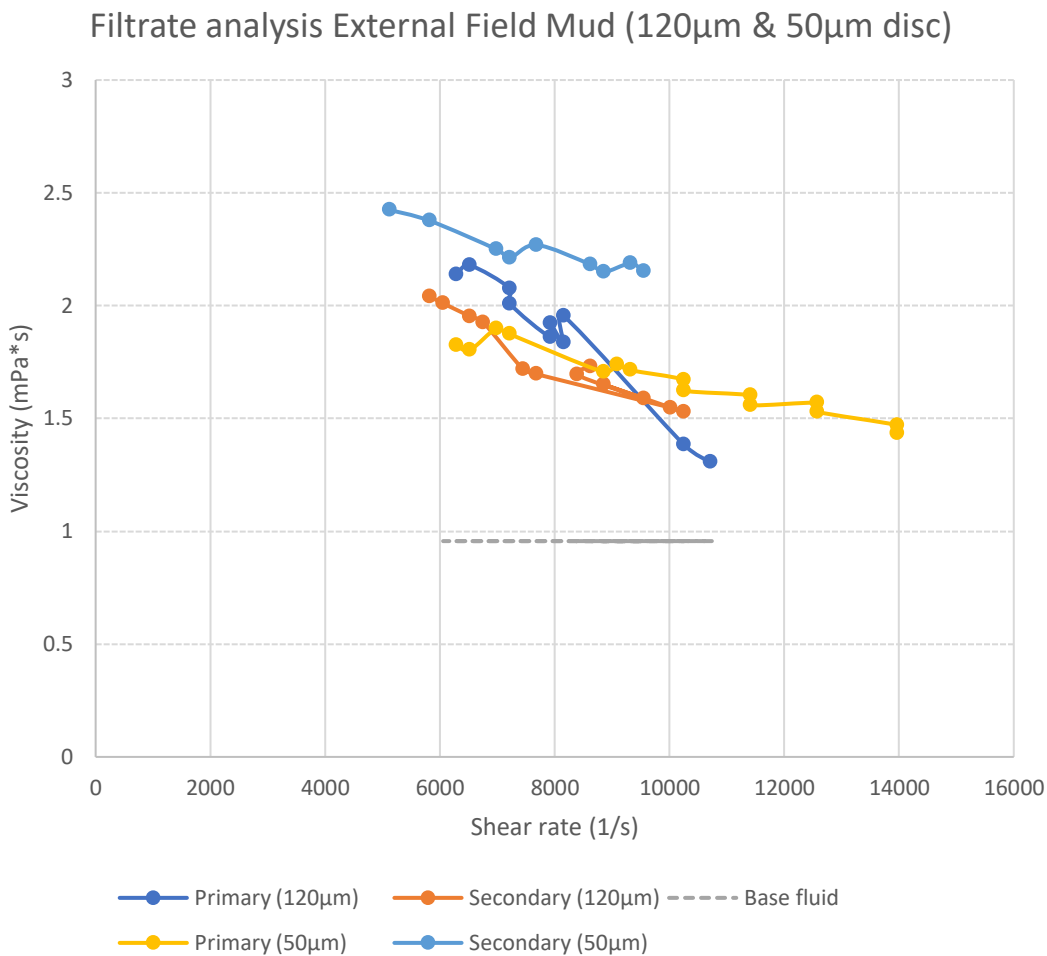


Figure 15: Shear rate versus Viscosity for external Field Mud, Sample 10 (120 $\mu\text{m}$ ) and Sample 12 (50 $\mu\text{m}$ )

By separating the filtrates from the *Field Mud* on two ceramic discs with different median pore size, the results show a different story compared to the tests conducted on 22 $\mu\text{m}$  filter paper. Both of these samples resulted in significantly higher spurt loss and total fluid loss compared to filter paper tests. Which is not surprising with now larger pore sizes. The four filtrates have a noticeable slowly shear thinning trend upon increasing shear rate. But the respective primary and secondary filtrates, are not as clearly separated. *Secondary (50 $\mu\text{m}$ )* resulted in the most viscous filtrate. This might be explained by the large volume of fluid loss compared to the same fluid tested on 22 $\mu\text{m}$  filter paper. With now more dispersed particles and polymers in both filtrates. Another reason is that the total fluid loss is relatively low, and



the pre – wetting fluid gets displaced. When the HTHP effect kicks in, and the spurt loss goes through the disc, the pre – wetting medium (water) might have an effect and join the primary filtrate on some occasions. This is not the case with the filter paper tests conducted, as they were not pre – wetted.

By looking at the Y-axis in **figure 15**, it is observed that all of the viscosity calculations lie between a relatively small interval. Another observation is that the *Field Mud* filtrate analysis on 22 $\mu$ m, clearly resulted in a more viscous primary filtrate with pseudo-plastic behavior, with a Newtonian behaving secondary filtrate. *Sample 12* presents now a more viscous secondary filtrate compared to the spurt loss, with no clear signs of a Newtonian behavior. The disc mass increase of only 0,017g for *sample 10* and 0,002g for *sample 12*, results in little formation damage. Which indicates that almost all the particles went through the pores and ended up as filtrate, but also provided filter cake development.

### 3.4.2 Filtrate analysis of external LAB Mud (160µm, 120µm, 180µm & 10µm disc)

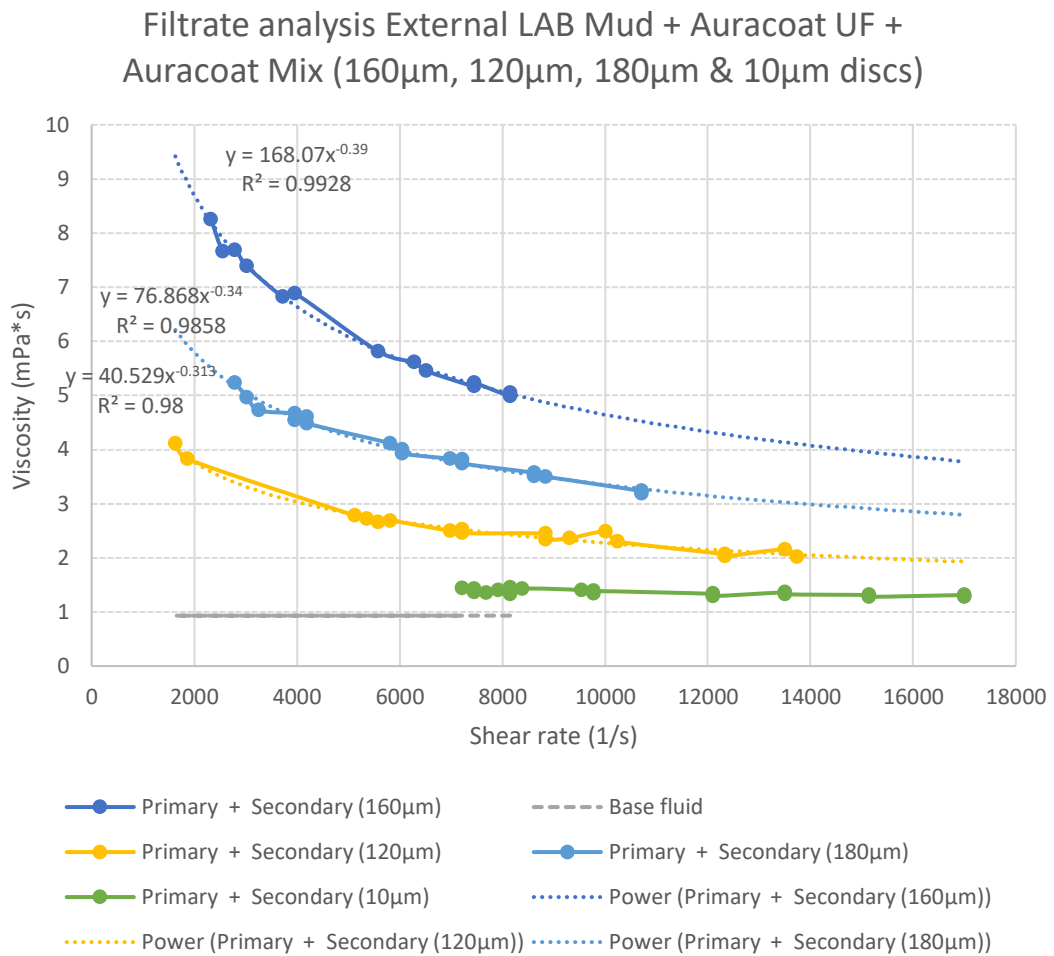


Figure 16: Shear rate versus Viscosity for combined filtrate of External LAB Mud + Auracoat UF + Auracoat Mix for Sample 15 (160µm), Sample 16 (120µm), Sample 17 (180µm) and Sample 18 (10µm) with additional power law trendline for Sample 15 (160µm, Sample 16 (120µm) and Sample 17 (180µm).

Figure 16 presents the combined filtrate following HTHP fluid loss test conducted on 120, 160, 180 and 10µm discs. With *sample 16 (120µm)* and *sample 18 (10µm)* containing 2 ppb more added Auracoat Mix compared to the two other samples. This increase in larger cellulose based particles resulted in a much more controlled and reduced fluid loss compared to *sample 15 (160µm)* and *17 (180µm)*.

The results in **figure 16** show a clear decreasing viscosity trend upon increasing shear rate for the filtrates from the 160, 180 and 120 $\mu\text{m}$  discs. The well distributed filtrates suggests significantly more viscous filtrates compared to the reference viscosity of the base fluid at a measured 23°C. Highly substantiated by the strong goodness of fit of the trendlines, with a value of 0,9928 for *sample 15*, 0,98 for *sample 16* and 0,9858 for *sample 17*. Strongly implying power law fluids. For the filtrate from the 10 $\mu\text{m}$  disc, did the reduction of the median pore sized disc have an interesting effect on viscosity. By evaluating **figure 16**, does the combined filtrate not show a distinct shear thinning effect as the others. It clearly has a distinct Newtonian behavior. The standard deviation of the viscosity calculations for this filtrate was 3,9 %. Upon increasing shear rate, does the filtrate show extremely little divergence. Hence indicating that the viscosity might only be dependent on temperature change. Additionally, did the filtrate result in a viscosity not far away from the reference of the base fluid. Only a 37 % difference separated the average viscosity measurements, and the reference of base. As observed in **figure 17**, could the *sample 18* (10 $\mu\text{m}$  disc) filtrate unscientifically be deemed as transparent. Suggesting a low viscous filtrate. Furthermore, does also *sample 16* show a clearer filtrate with less particles upon inspection, compared to *sample 15* and *17* which had less large sized cellulose based particles added. The 120 $\mu\text{m}$  disc ended up with a 0,048 g mass increase, with the 10 $\mu\text{m}$  disc increasing with 0,027 g, which is a drastically lower indicator of formation damage, compared to the two other discs presented in this section. Meaning an improvement in sealing capabilities. Both *sample 16* (120 $\mu\text{m}$  disc) and *sample 18* (10 $\mu\text{m}$  disc) built a smooth and relatively thick filter cake as presented in **figure 17**.

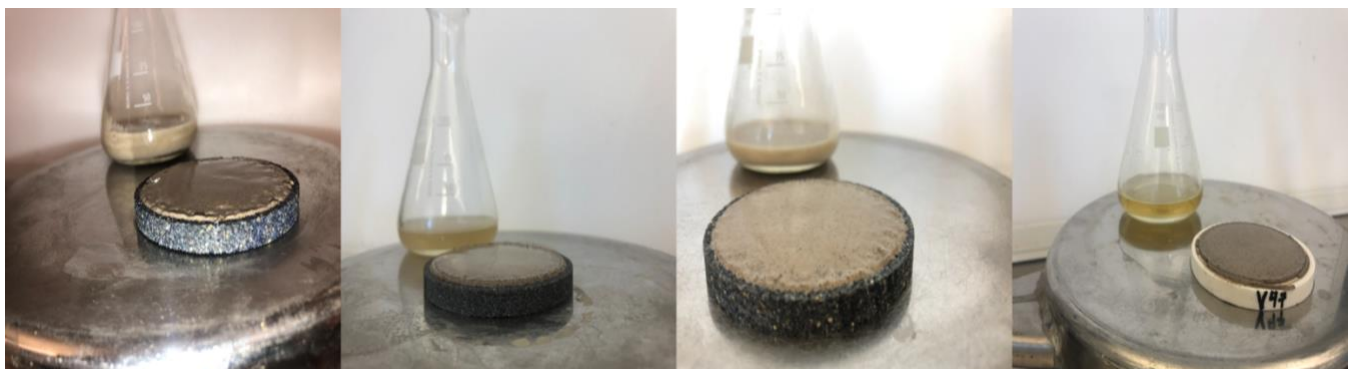


Figure 17 : From left to right, combined Primary + Secondary filtrate for LAB Mud + AUF + AUX, with respective filtercake for Sample 15 – 18. From left to right - 160 $\mu\text{m}$ , 120 $\mu\text{m}$ , 180 $\mu\text{m}$  and 10 $\mu\text{m}$  discs.

## 4 Conclusion

By optimizing the testing conditions as much as possible to simulate actual conditions, and applying different procedures for drilling fluid research, the data obtained can be used to better understand fluid loss. Further, it may provide insight into how different additives may seal high permeable formations. Based on the results, the conclusions and key findings of this study were:

- The tests conducted, provided consistent results with regards to RPF and disc mass increase.
- Tests on 2,5 $\mu$ m filterpaper does not differentiate the capabilities of drilling fluid with regards to sealing high permeability formations.
- When the filtercake has been established for tests conducted on 22 $\mu$ m filter paper, the secondary filtrate for OBM is nearly base oil. Equivalently for the water based fluids, the secondary filtrate is close to water.
- There were clear distinctions in primary and secondary filtrate from 22 $\mu$ m filterpaper tests. With the spurt loss phase (primary filtrate) generating potential formation damage due to the invasion of polymers and fine particles.
- It was a clear viscosity connection between the secondary filtrate and the base fluid from 22 $\mu$ m filter paper tests.
- The addition of ultra fine cellulose based particles gave good results when it comes to prevention of loss of fluid, and formation damage for a wide range of discs and filter papers with different median pore size.
- The results suggests that a continuous addition of large particle sized CaCO<sub>3</sub> to the fluid, would increase the viscosity of the primary filtrate upon increased shear rate, hence increase the risk of formation plugging as the particles grind down.
- There were observed small differences in the choice of best fitted regression model on viscosity profiles for selected filtrates. Power, exponential, and logarithmic models did all show acceptable trends.
- The key finding was that the primary filtrates often showed shear thinning properties, whereas secondary filtrates showed Newtonian properties.
- The fluid filtrate analysis conducted with 22 $\mu$ m filterpaper may yield insight into formation damage caused by the drilling fluid, although specific measurements of changes in permeability cannot be conducted.

- The addition of various sized cellulose based particles improved the sealing capabilities of the drilling fluid also after exposure to mechanical wear. In contrast, fluids with CaCO<sub>3</sub> as the main fluid loss additive showed significantly reduced sealing ability after exposure to mechanical wear.

## 5 References

1. Guan, Z., Chen, T., Liao, H. (2021). Well Control. In: *Theory and Technology of Drilling Engineering*. Springer, Singapore. [https://doi.org/10.1007/978-981-15-9327-7\\_6](https://doi.org/10.1007/978-981-15-9327-7_6)
2. Klungtvedt, K. R., & Saasen, A. (Dec 2022) Comparison of Lost Circulation Material Sealing Effectiveness in Water-Based and Oil-Based Drilling Fluids and Under Conditions of Mechanical Shear and High Differential. *Journal of Energy Resources Technology*. Vol.144, Issue 12
3. Ba Geri, B. S., Al-Mutairi, S. H., Mahmoud, M. A., Different Techniques for Characterizing the Filter Cake. (2013) *Paper presented at the SPE Unconventional Gas Conference and Exhibition, Muscat, Oman, January 2013*.  
<https://doi.org/10.2118/163960-MS>
4. Li, D., He, W., Journey Into Filter Cakes: A Microstructural Study (2015). *Paper presented at the International Petroleum Technology Conference, Doha, Qatar, December 2015*. <https://doi.org/10.2523/IPTC-18246-MS>
5. Civan, F. Reservoir Formation Damage (2020), *Gulf Professional Publishing: Waltham, MA, USA*, 2020; pp. 1–6, ISBN 978-0-12-801898-9.
6. Norsok, 2013, D-010, “Well integrity in Drilling and Well Operations,” Standards Norway, Rev 4.
7. Klungtvedt, K.R., Saasen, A. « The Role of Particle Size Distribution for Fluid Loss Materials on Formation of Filter- Cakes and avoiding Formation Damage”, *Journal of Energy Resources Technology*, April 2023 Vol.145., DOI: 10.1115/1.4056187
8. Klungtvedt, K. R., Saasen, A., 2022, « A Method for Evaluating Drilling Fluid Induced Permeable Formation Damage,” *Journal of Petroleum Science Engineering*, 213, p. 110324
9. Alvi, M. A. A., Belayneh, M., Fjelde, K. K., Saasen, A., and Bandyopadhyay, S., 2020, “Effect of Hydrophobic Iron Oxide Nanoparticles on the Properties of Oil-Based Drilling Fluid,” *ASME Journal of Energy Resources Technology*., 143(4), p. 043001
10. Nelson, P.H., 2009. Pore-throat sizes in sandstones, tight sandstones and shales. *Am. Assoc. Petrol. Geol. Bull.* 93, 329–340. NO. 3 (March 2009).

11. Klungtvedt, K.R., Saasen, A., Vasshus, J. K., Trodal , V. B., Mandal , S. K., Berglind, B., Khalifeh, M., 2021, «The Fundamental Principles and Standard Evaluation for Fluid Loss and Possible Extensions of Test Methodology to Assess Consequences for Formation Damage,” *Energies*, 18(8), p. 2252
12. Bergsvik, I. S., (2022). Optimizing formulations for reservoir drilling fluids. *Bachelor thesis for University of Stavanger*.

## Appendix A – Recipes

Appendix A includes the recipes for mixing the different fluids. **Table A1** will include the components and mixing order for the *WBM (sample 1-2)*. **Table A2** will present the components and mixing order for the *OBM (sample 3-4)*. Since the foundational components of the two externally acquired water based drilling fluids (*sample 5-18*) were unknown, will the relevant additives for the samples be presented in **Table A3**.



Table A1: Recipe and mixing progression of WBM + XF + Auracoat UF + Auraseal + 3.6  $\mu\text{m}$   $\text{CaCO}_3$  (Sample 1-2).

Mixing order	Component	Amount	Duration of mixing
1	Water, $\text{H}_2\text{O}$ , Hydrogen oxide	317,2g	
2	Soda ash, $\text{Na}_2\text{CO}_3$ , Sodium carbonate	0,02g	10s
3	Caustic soda, $\text{NaOH}$ , Sodium hydroxide	0,25g	10s
4	Xanthan gum, XC (Barazan)	1,5g	5min
5	Polymer (N-Dril HT Plus)	2g	5min
6	Starch (Dextride – E)	5g	5min
7	$\text{MgO}$ , Magnesium oxide	1g	30s
8	Salt, $\text{NaCl}$ , Sodium chloride	20g	1min
9	Auracoat Ultra fine (UF)	4,25g	1min
10	$\text{CaCO}_3$ , Calcium carbonate (3,6 $\mu\text{m}$ )	20g	1min
11	$\text{CaCO}_3$ , Calcium carbonate, Trucarb 10 (10 $\mu\text{m}$ )	10g	1min
12	Auraseal	5,25	1min
13	XF cellulose	0,75g	5min

Table A2: Recipe and mixing progression of OBM (Sample 3-4).

Mixing order	Component	Amount	Duration of mixing
1	Base oil SIP dril 4.0	189,64g	20min
1	Organophilic clay	6,5g	
2	Primary emulsifier	5g	10min
2	Secondary emulsifier	7g	
2	Lime, $Ca(OH)_2$	7g	
3	$CaCl_2$ Brine 30 %	98,33g	10min
4	Gilsonite	4g	5min
5	Organophilic lignite	2g	5min
6	$CaCO_3$ , Calcium carbonate (50/50<53 & D50=50 $\mu$ m)	40g	5min

Table A3: External drilling fluids (Sample 5-18) with respective additives.

Sample.nr	Description	Additive 1	Additive 2
5	External Field Mud	-	-
6	External Field Mud + Dextride-e + AUF	4g Dextride - e	4g Auracoat UF (D90=75µm)
7	External LAB Mud	-	-
8	External LAB Mud	4g Auracoat UF (D90=75µm)	5g Auracoat Mix (75-200µm)
9	External LAB Mud	4g Auracoat Medium (D90<150µm)	-
10	External Field Mud	-	-
11	External Field Mud	-	-
12	External Field Mud	-	-
13	External LAB Mud	-	-
14	External LAB Mud	4g Auracoat UF (D90=75µm)	-
15	External LAB Mud + AUF + AUX	4g Auracoat UF (D90=75µm)	3g Auracoat Mix (75-200µm)
16	External LAB Mud + AUF + AUX	4g Auracoat UF (D90=75µm)	5g Auracoat Mix (75-200µm)
17	External LAB Mud + AUF + AUX	4g Auracoat UF (D90=75µm)	3g Auracoat Mix (75-200µm)
18	External LAB Mud + AUF + AUX	4g Auracoat UF (D90=75µm)	5g Auracoat Mix (75-200µm)

## Appendix B – Relevant calculations

The following formulas were used for calculations of the different parameters for fluid loss and filtrate analysis:

$$FL_T = C_{FL} * T^{0,5} + SL, \quad \text{where}$$

$FL_T$  is the fluid loss (mL)

$C_{FL}$  is the coefficient of fluid loss

$T^{0,5}$  is the square root of time

$SL$  is the spurt loss constant (mL)

$$RPF = \frac{SL}{C_{FL}}, \quad \text{where}$$

$RPF$  is the relative plugging factor

$SL$  is the spurt loss constant (mL)

$C_{FL}$  is the coefficient of fluid loss

$$M_{Change} = M_a - M_b, \quad \text{where}$$

$M_{Change}$  is the change in disc mass

$M_a$  is the disc mass before fluid loss test (g)

$M_b$  is the disc mass after fluid loss test (g)

$$\rho_f = \frac{M_f}{V_f}, \quad \text{where}$$

$\rho_f$  is the fluid filtrate density ( $\frac{kg}{m^3}$ )

$M_f$  is the mass of the filtrate (kg)

$V_f$  is the volume of the filtrate ( $m^3$ )

$$R_e = \frac{64}{f}, \quad \text{where}$$

$R_e$  is the Reynolds number

$f$  is the Darcy friction for laminar flow

$$\mu = \frac{\rho_f \times U_n \times D}{R_e}, \quad \text{where}$$

$\mu$  is the calculated viscosity ( $Pa \times s$ )

$\rho_f$  is the fluid filtrate density ( $\frac{kg}{m^3}$ )

$U_n$  is the fluid velocity in needle ( $\frac{m}{s}$ )

$D$  is the diameter in needle (m)

$R_e$  is the Reynolds number

$$U_n = \frac{\frac{Q}{1000}}{\frac{60}{\left(\frac{3,1415 \times D}{2}\right) \times \left(\frac{D}{2}\right)}}, \quad \text{where}$$

$U_n$  is the fluid velocity in needle ( $\frac{m}{s}$ )

$Q$  is the measured flow ( $\frac{l}{min}$ )

$D$  is the diameter in needle (m)

$$\gamma = 8 \times \frac{U_n}{D}, \quad \text{where}$$

$\gamma$  is the shear rate ( $\frac{1}{s}$ )

$U_n$  is the fluid velocity in needle ( $\frac{m}{s}$ )

$D$  is the diameter in needle (m)

$$U_c = \frac{\frac{Q}{1000}}{\frac{60}{(3,1415 \times 0,00475 \times 0,00475)}}, \quad \text{where}$$

$U_c$  is the calculated velocity in container ( $\frac{m}{s}$ )

$Q$  is the measured flow ( $\frac{l}{min}$ )